

TECHNICAL MEMO 08-035



Seismic Array Directionality Study

Jesse Spence

July 28, 2008

NCE JOB No. J08-040

Prepared for:

Stress Engineering Services, Inc.

13800 Westfair East Dr.

Houston, TX 77041

Attention: Mr. Ray Ayers

Prepared by:

NOISE CONTROL ENGINEERING, Inc.

799 Middlesex Turnpike

Billerica, MA 01821

978-670-5339

978-667-7047 (fax)

nonoise@noise-control.com

<http://www.noise-control.com>

TABLE OF CONTENTS

LIST OF FIGURES..... III

0.0 EXECUTIVE SUMMARY 1

1.0 INTRODUCTION 4

2.0 AIR BUBBLE CURTAIN 4

 2.1 BACKGROUND 4

 2.2 MODELING 5

 2.3 RESULTS..... 6

 2.3.1 2-D Deep Water..... 6

 2.3.2 2-D Shallow Water..... 9

 2.3.3 3-D Deep Water..... 10

 2.4 CONCLUSIONS – BUBBLE BARRIER..... 11

3.0 LOW IMPEDANCE BARRIER MATERIALS 13

4.0 PARABOLIC REFLECTOR 14

 4.1 BACKGROUND 14

 4.2 MODELING 15

 4.3 RESULTS..... 16

 4.4 CONCLUSIONS - REFLECTOR..... 17

REFERENCES 17

LIST OF FIGURES

FIGURE 1: THEORETICAL AND MEASURED SOUND SPEED IN AIR-WATER MIXTURE VS. AIR
CONTENT 18

FIGURE 2: UNDERWATER AIR CURTAIN BARRIER CONCEPT 19

FIGURE 3: EXAMPLE ARRAY DESIGN 20

FIGURE 4: EXAMPLE 2-D DEEP WATER MODEL..... 20

FIGURE 5: EXAMPLE 2-D SHALLOW WATER MODEL 21

FIGURE 6: EXAMPLE 3-D DEEP WATER MODEL..... 21

FIGURE 7: DIRECTIVITY FOR 2-D DEEP WATER MODEL, NO BARRIER..... 22

FIGURE 8: BARRIER EFFECT FOR 2-D DEEP WATER MODEL, BASELINE BARRIER..... 22

FIGURE 9: LP IN DB, 2-D DEEP WATER MODEL, BASELINE BARRIER, 30 HZ 23

FIGURE 10A: LP IN DB, 2-D DEEP WATER MODEL, BASELINE BARRIER, 600 HZ..... 24

FIGURE 10B: COMPARISON OF LP FOR BASELINE BARRIER VS. NO BARRIER, 600 HZ, 2-D DEEP
WATER MODEL..... 25

FIGURE 11: BARRIER EFFECT FOR 2-D DEEP WATER MODEL, DEEP BARRIER 25

FIGURE 12: BARRIER EFFECT FOR 2-D DEEP WATER MODEL, SHALLOW BARRIER 26

FIGURE 13: BARRIER EFFECT FOR 2-D DEEP WATER MODEL, CLOSE BARRIER 26

FIGURE 14: BARRIER EFFECT FOR 2-D DEEP WATER MODEL, FAR BARRIER 27

FIGURE 15: BARRIER EFFECT FOR 2-D DEEP WATER MODEL, LOW SATURATION BARRIER..... 27

FIGURE 16: BARRIER EFFECT FOR 2-D DEEP WATER MODEL, THIN BARRIER 28

FIGURE 17: BARRIER EFFECT FOR 2-D DEEP WATER MODEL, OPTIMIZED..... 28

FIGURE 18: SOUND LEVEL IN DB, 2-D SHALLOW WATER (30 METER) MODEL, NO BARRIER, 600 HZ..... 29

FIGURE 19: BARRIER EFFECT FOR 2-D SHALLOW WATER MODEL, 20 METER DEPTH 29

FIGURE 20: BARRIER EFFECT FOR 2-D SHALLOW WATER MODEL, 30 METER DEPTH 30

FIGURE 21: 2-D MODEL RESULTS FOR BASELINE BARRIER VS. PRESSURE RELEASE SURFACE 30

FIGURE 22: COMPARISON OF 3-D VS. 2-D MODEL RESULTS..... 31

FIGURE 23: PLOT OF RESULTS EXTRACTION LOCATIONS..... 31

FIGURE 24: BARRIER EFFECT FOR 3-D MODEL, 100 HZ..... 32

FIGURE 25: BARRIER EFFECT FOR 3-D MODEL, 200 HZ..... 32

FIGURE 26: CONCEPT SKETCH OF PARABOLIC REFLECTOR..... 33

FIGURE 27: EXAMPLE PARABOLIC REFLECTOR MODEL..... 33

FIGURE 28: LATERAL DIRECTIVITY FOR SINGLE LINE AIR GUN ARRAY, 3 METER DEPTH, NO
REFLECTOR 34

FIGURE 29: REFLECTOR EFFECTIVENESS, 3 METER DEEP ARRAY, LARGE REFLECTOR 34

FIGURE 30: REFLECTOR EFFECTIVENESS, 3 METER DEEP ARRAY, MEDIUM REFLECTOR..... 35

FIGURE 31: REFLECTOR EFFECTIVENESS, 3 METER DEEP ARRAY, SMALL REFLECTOR..... 35

FIGURE 32: REFLECTOR EFFECTIVENESS, 6 METER DEEP ARRAY, SMALL REFLECTOR..... 36

FIGURE 33: REFLECTOR EFFECTIVENESS, 3 METER DEEP ARRAY, MEDIUM REFLECTOR, 30 METER
DEEP WATER (SHALLOW)..... 36

FIGURE 34: REFLECTOR EFFECTIVENESS, 3 METER DEEP ARRAY, MEDIUM REFLECTOR, PRESSURE
RELEASE SURFACE..... 37

0.0 EXECUTIVE SUMMARY

Noise Control Engineering (NCE) has performed a study to identify possible methods of reducing lateral sound propagation from air gun arrays. The methods investigated here include 1) use of a longitudinally-oriented air bubble curtain on both sides of the air gun array, 2) use of a barrier made of a low acoustic impedance material in a similar configuration to item 1, and 3) use of a parabolic reflector to focus sound downwards. This study has been performed using the Comsol™ finite element modeling software which contains an integrated acoustics module for modeling wave propagation around complex structures.

All three concepts appear to have merit and may be capable of reducing lateral transmission of sound. In general, the effectiveness of any of these approaches is dependent on the air gun array details, such as gun sizes, depth in the water, and configuration. Such factors must be taken into account when assessing the performance or making recommendations regarding optimal configurations of a barrier or reflector. Furthermore, the models used in this study are idealized, and the results should be taken as approximate. While the results indicate that all of the approaches are worth further consideration, testing a prototype is recommended to get a better determination of real-world effectiveness. This testing will also allow for feasibility studies of non-acoustic issues which are not addressed in detail in this report.

A summary of the results for each treatment is provided below.

Bubble Curtain Barrier

The air bubble curtain concept is shown in Figure 2. In deep water, it has been shown that reductions in sound with a bubble barrier are possible at 100 Hz and above for angles greater than 50 degrees relative to the vertical axis (i.e. near the water surface) for receivers that are located on the side of the air gun array ('lateral' or 'transverse' direction). Reductions of 5-25+ dB have been seen in some cases, though the performance is frequency dependent and does not necessarily get better at higher frequencies.

The effectiveness of the barrier is dependent on various parameters such as depth, distance from centerline, and air content. It has been shown that maximum effectiveness at higher frequencies can be achieved by locating the barrier as close to the air gun array as possible. Deeper barriers will also improve performance; though there will be diminishing returns below a certain depth. The bubble curtain should contain at least 10% air by volume. Barrier thickness does not appear to be a dominant factor in performance.

A longitudinal barrier will not significantly change the directivity of the array on centerline (fore/aft direction). For air gun arrays that have larger air guns near the front, the barrier effectiveness appears to be good for transverse propagation and propagation at forward azimuth angles (i.e. angles in the forward direction in the plane of the water surface). Effectiveness will drop off more rapidly for aft azimuth angles. The barrier length should generally be made as long as possible to maximize effectiveness, though some effectiveness is possible even for barriers that are short relative to the length of the air gun array.

Amplifications of sound should also be expected at some angles over certain frequency ranges. The specific angle where amplifications occur depend on the specific frequency, barrier configuration, and air gun arrangement, though amplifications as high as 20 dB have been seen.

There is also a potential for a reduction in sound at frequencies below 100 Hz directly beneath the array. While most frequencies below 100 Hz were largely unaffected by the barrier, some configurations showed reductions of sound as high as 12 dB directly below the array at specific frequencies (i.e. 30 Hz). This is an important result as these frequencies are useful in identifying geological features beneath the sea floor.

If the barrier is used in shallow water (~20-30 meters) then the reflections off the sea floor will act to reduce the effectiveness of the barrier. If the bottom is assumed to be 'perfectly rigid,' all frequencies are seen to have significant reductions in effectiveness, and some frequencies are not attenuated at all. For realistic sea floors it is expected that the reduction in performance would not be quite this dramatic, though the results will depend on the specific makeup of the sea floor and the amount of sound that is absorbed.

Low Impedance Material Barrier

It is possible to use closed cell foam materials in place of an air bubble curtain for the above barrier design, or for the parabolic reflector. Soft foam materials such as nitrile, neoprene, EPDM, etc. should work well from an acoustical perspective, and can be rolled for efficient retrieval, storage, and deployment. However, these materials may create added drag due to oscillatory lateral motion as they are pulled through the water (i.e. motion similar to a flag blowing in the wind). Additional structures are likely to be necessary in order to support these materials and to ballast the barrier into position.

Rigid closed cell foams such as polyurethane foam can also be used for these applications, though the specific properties should be assessed prior to use. Rigid foams will have the advantage of maintaining their shape in the water, potentially requiring less hardware to maintain position. However, hard foams will be more difficult to deploy and retrieve.

The modeling of the air bubble barrier (and reflector, see below) indicates that the acoustic effectiveness is not affected by the thickness of the barrier. However, it is reasonable to assume that if a foam material is used then there will be some thickness below which effectiveness will drop off. By analyzing the particle velocity in a material that has a specific acoustic impedance 30 times less than water, it has been estimated that the minimum required thickness of the barrier would be 1 inch assuming a sound pressure level of 210 dB re 1 μ Pa at the barrier. Higher sound pressure levels may require thicker materials. Testing is recommended to confirm this assumption.

Parabolic Reflector

The parabolic reflector concept has a potential for large reductions in sound, particularly at vertical angles greater than 70 degrees. Compared to the effectiveness of the vertical barriers discussed above, the reflector appears to provide similar or greater reductions in sound over a larger vertical angle. A concept sketch of this design is provided in Figure 26. The air gun array has been modified for this design; a single longitudinal line of air guns is used instead of

multiple lines as is commonly used. Note that this configuration would provide additional longitudinal (centerline) directivity relative to a multiple line array if the same number of air guns is used.

The reflector is seen to provide an increase in output directly below the array of up to 10 dB for most frequencies, though the lowest frequencies (5, 30 Hz) can have reductions in sound of up to 17 dB.

The shape of the reflector has been selected so that the air gun array is located at the focus of the parabola. This means that arrays located closer to the water surface will tend to require less surface area for a given performance. For arrays located deeper in the water the size of the reflector may be a practical limitation. If air bubbles are used to make the reflector, the hoses used to create the air bubble curtain must be oriented laterally (transverse), and many rows of hoses must be used in order to maintain the parabolic shape over the entire array. This may prove difficult in practice. A solid material may be preferable in this case, and would also provide similarly large sound level reductions. Such a reflector would likely need to be assembled in sections to cover the entire length of the array.

As was found for the barrier designs, the effectiveness in shallow water is significantly compromised as a result of bottom reflections. If the sea floor is absorptive then this reduction in performance may not be as dramatic.

1.0 INTRODUCTION

Noise Control Engineering (NCE) has performed a study of various potential methods to reduce lateral propagation of sound from an air gun array used for seismic exploration. The purpose of this study is to identify feasible approaches for blocking lateral sound propagation to protect marine life that may exist near seismic survey operations. The study focuses on three approaches: 1) use of a longitudinally oriented air bubble curtain on both sides of the air gun array, 2) use of a low acoustic impedance material as a curtain in a similar configuration to item 1, and 3) use of a parabolic reflector to focus sound downwards. This study has been performed using the Comsol™ finite element modeling software which contains an integrated acoustics module for modeling wave propagation around complex structures.

Section 2 of this report discusses the models and results of the air bubble curtain analysis. Section 3 discusses possible materials that could be used for a barrier. Section 4 discusses the model and results of the parabolic reflector analysis.

2.0 AIR BUBBLE CURTAIN

2.1 Background

Air bubbles have been used in many applications to block underwater sound from pile driving and explosives [1]. The principle mechanism driving sound attenuation is the impedance mismatch between the water and the bubble curtain's air-water mixture. Reference [2] provides measurements of acoustic wave speeds in an air-water mixture for various levels of air saturation. A plot showing theoretical and measured results is provided in Figure 1. From this curve it is seen that introducing 10% air by volume reduces the speed of sound from approximately 1500 m/s to 45 m/s. This results in an impedance drop (density * speed of sound) from 1.5e6 rayls to 4.5e4 rayls, a factor of 33. This large impedance difference results in a strong reflection of sound waves at the bubble curtain boundary, and transmission through the bubble curtain is minimized.

Bubble curtains used for mitigating sound from pile driving and explosives must extend through the entire water column and completely surround the noise source in order to achieve any effectiveness (applications are limited to shallow water). Attenuations can vary depending on the specifics of the installation and ground conditions, but reductions in peak pressure, RMS pressure, and energy of 5-20+ dB have been documented [1].

Creating a bubble curtain that extends through the entire water column for a moving seismic source is not a practical endeavor. However, an attempt to use a bubble curtain as a barrier for a seismic source has been documented in Reference [3]. A sketch of the concept design is provided in Figure 2. The original intention of this design was to reduce interference at the receiving hydrophone array from shallow water acoustic modes; the seismic signal was being degraded by reinforcement of the reflected signal (in the water) at some frequencies. It was suggested in [3] that this approach may also be beneficial for reducing sound impacts on marine life.

Barriers have been used extensively on land for industrial and residential noise control [4]. The use of a barrier for underwater purposes is similar in concept, although some differences exist. If a bubble curtain is used, the barrier itself will be a pressure release surface rather than a hard

surface. Similarly, the ‘ground’ plane is a hard surface in air applications where it is a pressure release surface in water. These differences will change the way sound propagates in the medium, and will have impacts on the effectiveness of the barrier as is discussed in later sections. It is also worth noting that the speed of sound is very different in air vs. water, and therefore the effective frequency ranges will be different as well for a given geometry. The current study investigates the feasibility of the air curtain barrier approach with expected sound reductions at different frequencies.

2.2 Modeling

An arbitrary though practical array design was selected as a basis for this analysis, as shown in Figure 3 (based on Reference [5]). The air gun volumes are shown in this figure. It is indicated in Reference [3] that the acoustic pressure of an air gun is related to the cube root of the volume. The air guns are assumed to be positioned 3 meters below the waterline. The seismic vessel itself was not included in this analysis in order to reduce model size.

Several models were created as part of this analysis. The initial study was performed using two-dimensional models in order to decrease model size and allow for faster solution times and parameter investigation. While this analysis ignores the fore-aft component of the propagation, longitudinal barrier extent, and longitudinal details of the array, it does provide insight into appropriate parameters for the bubble curtain.

Examples of some 2-D models are shown in Figures 4 and 5. Figure 4 represents an array in deep water where bottom reflections are of secondary importance and Figure 5 represents an array in shallow water. All models use half symmetry along the vertical-CL plane. The air gun array was modeled as two point (line) sources. Given the relative sizes (pressure output) of the air guns on centerline vs. off centerline in Figure 3, the centerline air gun pressure was assigned to be 1.08 times the pressure of the off centerline air gun. This relationship holds for the forward three air gun sets and deviates slightly for the aft three.

The water was modeled with a density of 1000 kg/m^3 and a speed of sound of 1500 m/s . Some variation in these values will occur for different locations (resulting from temperature, depth, etc.), though these variations are small relative to the size of the model, and the expected differences in directivity results are small over short distances. The top surface of the model was set to be a pressure release surface. The outer portion of the model is a “Perfectly Matched Layer” (PML), which is a construct of Comsol™ that is used to accurately model an ‘infinite’ boundary (i.e. no reflection occurs beyond the inner surface of the PML).

The barrier itself was modeled using various properties, locations, and sizes. The speed of sound and density of the barrier was modeled using various data points from Figure 1. Locations off centerline ranged from 9 meters to 20 meters (note that the half width of the modeled array is 8 meters), and the depth ranged from 9 to 20 meters. Barrier thickness ranged from 0.0254 meters (1 inch) to 0.3 meters (12 inches), which is assumed to be the practical extent in practice. The air curtain was assumed to have uniform thickness throughout its depth. This is likely not to be the case as some spreading or movement is expected as the bubbles approach the water surface, though the extent of this spreading is not known. When modeled, the sea floor was assumed to

be a hard, reflecting surface. While this is obviously an approximation, the results from this analysis are instructive.

A harmonic (steady state) analysis was performed at discrete frequencies¹. The analysis frequencies for all 2-D models are 5, 30, 60, 100, 200, 400, and 600 Hz. Sound Pressure Level (Lp) results were extracted at a large distance from the model center approximating the far field level. Results were compared to the sound pressure level that occurs without a barrier, and a 'barrier effect' was created for both shallow- and deep-water models.

Some 3-D models were created as well, though these models were limited in frequency range due to their large model size. An example model is shown in Figure 6. Only deep-water models were analyzed in 3-D. The overall modeling approach was the same as for the 2-D models, though the full array shown in Figure 3 was modeled at discrete points with the appropriate (relative) source pressures. The longitudinal extent of the barrier was also modeled and the effects of modifying this extend were investigated.

2.3 Results

2.3.1 2-D Deep-Water

Before discussing the results of barrier effectiveness, it is important to establish the sound radiation from the modeled array without the barrier. Figure 7 shows the sound pressure level from the array (at a distance of 50 meters from the model center) vs. angle, with 0 degrees being vertical and 90 degrees being the water surface. The results have been normalized to the level at 0 degrees. It is clear that the directivity is strongly dependent on frequency². This is the expected result from an array of acoustic sources. However it is also important to note that even at low frequencies there is an apparent directivity because of the pressure release at the water surface. Another important aspect of these curves is the strong interference effects at the higher frequencies. The specific angles where the peaks and dips occur are related to the specific array layout and measurement distance. Changing these parameters will change the details of these curves, but the overall character would remain.

A 'baseline' barrier design has been defined for the purposes of this report as a barrier with the following properties: 12 meter depth, 12 meters off centerline, 0.1 meter thick, 45 m/s speed of sound, 900 kg/m³ density. This roughly corresponds to injection of 10% air by volume into the water. The effect of adding this barrier is shown in Figure 8 for various frequencies. Note that positive values on this graph represent a reduction in sound level. Several items can be initially identified from this data:

- There is minimal effect at very low frequencies at all angles (5 Hz). 60 and 100 Hz show small changes at angles near 0 degrees, and have some variation (<10 dB) at larger angles, both positive and negative.
- At 200 and 400 Hz there is a 10-30+ dB reduction at angles greater than 60 degrees. Smaller increases and decreases in sound are seen at lower angles.

¹ Although an air gun is inherently transient, a harmonic analysis is performed here to reduce analysis time and model complexity. On a frequency basis, the results should be the same as if a transient analysis is performed.

² Note that for a simple source in air with a hard floor, the directivity would be uniform with angle at all frequencies.

- At 30 Hz there is a 13 dB reduction of sound at 0 degrees. This gradually changes to a 0 dB reduction near 90 degrees.
- At 600 Hz there is a minimum 5 dB reduction in sound at angles between 71 and 87 degrees. There is also a 27 dB increase in noise at 56 degrees.

The non-effect at 5 Hz is to be expected because the wavelengths are very long at this frequency relative to the size of the barrier. At 30 Hz there is a reduction in sound directly below the array because of an interaction with the barrier. This interaction can be seen in Figure 9. The barrier itself is capable of supporting sound waves, and so there are certain wavelengths that will travel well within the barrier. This will cause effects similar to those seen in Figure 9 (i.e. local maxima and minima along the length of the barrier), leading to reductions in sound even at low frequencies. This is also the reason for the small differences in level at 0 degrees for other frequencies including 5, 60, and 100 Hz. This effect will occur to varying degrees at different frequencies for any barrier/array configuration; the specific amount of sound increase or decrease will depend on the details of the geometry and air gun array.

At higher frequencies (200 Hz and above) the curves begin to develop sharp peaks and dips. Note that the directivity of the array without a barrier also contains peaks and dips at these frequencies corresponding to constructive and destructive interference at the specific measurement locations (see Figure 7). Because these peaks and dips exist without a barrier, the barrier effectiveness curves will also have peaks and dips. A sharp dip in effectiveness, which may seem to indicate an amplification of sound, may result simply because the sound waves from the elements of the array destructively add at that location *without the barrier*, but add constructively with the barrier. The same can be said for sharp effectiveness peaks.

For reference, an example plot of the sound field at 600 Hz is provided in Figure 10a for the baseline barrier model. A comparison of the sound pressure level at 600 Hz with and without the baseline barrier is provided in Figure 10b. It is clear that in some cases, such as at 30 degrees, the destructive interference dips have shifted. This will cause an apparent performance decreases and increases near those angles. Since the spatially ‘quick’ variations are location specific, it is prudent to smooth sharp peaks and dips seen in Figure 8 such as the dip seen for 600 Hz at 56 degrees and the peak seen for 200 Hz near 76 Hz. Though not performed explicitly here, this smoothing allows for a general determination of the barrier effectiveness.

Using this approach, the following can be said about the baseline curtain design:

- At 200 Hz, there is an increase in sound of approximately 0-10 dB between the angles of 0-45 degrees, a decrease in sound of 0-10 dB between 45 and 60 degrees, and a 10 dB minimum decrease in sound between 60 and 90 degrees.
- At 400 Hz, there are small changes (positive and negative) from 0 to 52 degrees, and a 10-25 dB decrease in sound at larger angles.
- At 600 Hz, there are small changes (positive and negative) from 0 to 52 degrees, an increase in sound of approximately 8 dB near 55-67 degrees, and a 5+ dB decrease in sound at angles greater than 70 degrees.
- At 30 Hz there is a 13 dB reduction of sound at 0 degrees. This gradually changes to a 0 dB reduction near 90 degrees.

- There is generally minimal effect for other frequencies below 100 Hz, although some amplification is seen for large angles at 60 Hz. At 100 Hz the sound is reduced and amplified by less than 10 dB, depending on the angle.

Overall there appears to be some reduction in sound at frequencies above 100 Hz for angles over 70 degrees. However, some increases in sound at these higher frequencies can occur at smaller angles. Furthermore, frequencies in the range of useful seismic data (below 100 Hz) can be affected by the barrier.

When the barrier depth is changed, the effects noted above can be amplified or decreased. Increasing barrier depth improves the higher frequency attenuation at larger angles, but also amplifies the increase in sound at smaller angles. The deeper barrier also increases the reduction of sound at 30 Hz. A shallow barrier has the opposite effect. Figures 11 and 12 show the effectiveness for barriers with 20 and 9 meter depth, respectively (all other parameters are the same as for the baseline design). It is interesting to note that while changing the depth from 12 meters to 9 meters results in a large reduction in performance, the increase in performance by going from 12 meters to 20 meters is not as dramatic.

Changing the location of the barrier relative to centerline can also have an affect on performance. Figures 13 and 14 show the effectiveness for barriers located at 9 m OCL and 20 m OCL, respectively (all other parameters are the same as for the baseline design). Modifying the barrier location seems to increase barrier performance at some frequencies above 100 Hz while decreasing it for others. Again, this is due to the varying path lengths from the sources (and around the barrier) for a given receiver. Taking the aggregate performance for all frequencies above 100 Hz, the barriers positioned at 9 meters and 12 meters from the array have similar performance, with the 9 meter barrier having slightly better performance. The performance of the barrier positioned 20 meters from the array is certainly degraded. It is also worth noting that the 30 Hz reduction in sound seen with the 12 meter barrier is reduced for angles near 0 degrees. For this reason the 9 meter barrier would likely be preferable in this case.

Reducing the amount of air in the bubble curtain will reduce its performance. Figure 15 is a plot of the barrier effectiveness when the air content is dropped to 2% (density = 980 kg/m³, speed of sound = 150 m/s). Comparing this barrier with the baseline barrier, the high frequency attenuation at large angles is seen to have decreased. Interestingly, the 30 Hz reduction at 0 degrees has been replaced by a similar attenuation at 60 Hz. This again is due to the sound waves within the barrier itself. Increasing the air content to 30% (density = 700 kg/m³, speed of sound = 30 m/s) produces a large improvement at 400 Hz relative to the baseline case (where performance is already good) but minimal change at all other frequencies.

The effects of barrier thickness were also investigated. Figure 16 is a plot of the effectiveness of a barrier with a 0.0254 meter (1 in) thickness. All other parameters are identical to the baseline. Comparing this graph to the baseline effectiveness it is seen that there are only minor differences; the specific shape of the effectiveness curve at 400 Hz is different, but the overall trend is the same. The same can be said for the reduction in sound at 30 Hz. Other thicknesses showed similarly small impacts on the overall effectiveness. This implies that the thickness of

the barrier is not a dominant factor for barrier effectiveness, and that variations in thickness through the height of the barrier will only have minor impacts.

Taking the above results into account, an ‘optimized’ barrier was modeled (note that this is optimized for this array). Figure 18 shows the effectiveness of a barrier that is 9 meters from centerline, 20 meters deep, with 10% air by volume, 0.1 meters thick. The effectiveness is generally 10 dB or more at vertical angles of 70 degrees or more at 100 Hz and above. There is an amplification of sound at 400 Hz for vertical angles between 33 and 58 degrees, and the output at 30 Hz is reduced by 15 dB directly below the array. However, the overall performance of this barrier is significantly better than for the baseline case.

2.3.2 2-D Shallow-Water

The baseline curtain design discussed in the above section was modeled in 20 meter and 30 meter water depths. For both models the ocean floor was assumed to be a hard surface (i.e. perfect reflector). While this is certainly not the case in reality, it is assumed that this is something of a worst case approximation. The sea floor is likely to be closer to a hard ‘pressure doubler’ surface than a pressure release surface (such as the water surface), and some attenuation at certain frequencies is also possible. The specific properties of the sea floor will vary depending on location. The use of a hard surface for the sea floor is an approximation that should allow for general investigations to determine the effect of the presence of the sea floor.

As was the case for the deep-water models, the sound pressure level due to the array alone without a barrier can have significant variations that are dependent on location. This is due to the reasons given in the above section, as well as the existence of the ocean floor. An example plot of the sound pressure level at 600 Hz for the 30 meter water depth case is provided in Figure 18. Because of this, the sharp variations in barrier effect seen for the deep water case also exist here.

Figures 18 and 19 show the effectiveness of the baseline barrier in 20 and 30 meter water depths. Note that these graphs are plotted against water depth instead of angle as was the case for the previous graphs. All results are taken at a distance of 60 meters from centerline (i.e. measurement positions are along the right hand vertical edge of the model). At this distance the 30 meter water depth corresponds to a 63 degree angle and the 20 meter water depth corresponds to a 71 degree angle.

At 400 Hz, the reduction in sound is roughly 10 dB for both the 20 and 30 meter water depths, which is less effective relative to the deep water case (Figure 8). At 200 and 600 Hz there is, on average, no effectiveness for either depth. The overall reduction in effectiveness is primarily due to the scattering of sound from the bottom, and the modal pattern that arises. Because the bottom is modeled as a hard surface this is likely to be a worst case performance, but does indicate that the barrier effectiveness can be compromised by the presence of the sea floor.

It is interesting to note that at the 20 meter depth the 30 and 60 Hz frequencies are attenuated by 10 dB along the vertical plane at the right side of the model (representing the propagating sound wave). However, the sound pressure level directly below the array (not shown here) has also

been reduced by 10-20 dB. At 30 meters the 30 Hz sound is attenuated by approximately 10 dB as seen in the deep water case.

2.3.3 3-D Deep-Water

The number of finite elements required to model a 3-D space is very large compared to a 2-D space. Because of this, the frequency range that can be analyzed in 3-D is significantly smaller than for two-dimensional models³. To help reduce model size, the barrier was modeled at a distance of 9 meters from centerline as opposed to 12 meters in the 2-D baseline case. Furthermore, the barrier was modeled as a pressure release surface for all 3-D models. This is an approximation that appears to be valid for most frequencies assuming the bubble curtain has at least 10% air by volume. Figure 21 is a plot of the 2-D model baseline case vs. an identical model using a pressure release surface. At 100 and 200 Hz (and other frequencies not shown here) the results are very close. At 30 Hz the results do differ, but this is a result of the wave propagation within the barrier in the baseline model as discussed in Section 2.3.1. The current 3-D analysis focuses on waves at 100 and 200 Hz.

A comparison of the sound pressure level at 100 Hz between the 2-D and 3-D models is provided in Figure 22. This 3-D model uses a barrier that is 34 meters long with the other parameters the same as the 2-D baseline barrier with the exceptions noted above. The results of the 3-D model were taken along the transverse axis at the center of the array. The results are similar, and the small differences can be attributed to the differences in the modeling of the air gun array. Note that the air gun array is not symmetrical in the fore/aft direction, and therefore will not have exactly the same radiation pattern as a line source. This result is seen to verify the general findings of the 2-D modeling with regards to the effectiveness of the barrier and the effects of varying the barrier parameters. This result also underlines the fact that the specific performance of any barrier will be directly linked to the air gun array setup itself.

The effect of changing the barrier length was investigated, and the effective area of sound reduction in the fore/aft direction was analyzed. Sound pressure levels were extracted along the transverse or 'lateral' direction as well as along +/-45 degrees azimuth angles relative to the water surface, as shown in Figure 23⁴. Barriers with lengths of 34 meters, 20 meters, and 14 meters were modeled. The barrier was always centered longitudinally at the middle of the air gun array. Note that the array length is 15 meters.

The results at 100 Hz are presented in Figure 24. Of particular note is the fact that there is only moderate variation between the 34 and 20 meter barriers, and the 14 meter barrier actually appears to perform the best at this frequency. The barrier effectiveness is roughly 10 dB or more at (vertical) angles of 60 degrees or more (i.e. near the water surface) for the lateral and forward 45 degree azimuth angles. The large dip in the aft 45 degree azimuth line at the 63 degree

³ A rule of thumb of 8 elements per wavelength has been used here. With fewer elements, the highest frequency capable of analysis is reduced.

⁴ For the purposes of this report, spherical coordinates are used to identify locations in the 3-D model. The 'azimuth angle' refers to the angle away from the transverse direction in the plane of the water. 0 degrees azimuth would refer to the 'lateral' direction in Figure 22. The 'vertical angle' is the angle away from the vertical axis, with 0 degrees being directly below the air gun array. The center of the coordinate system is the middle of the air gun array at the water surface.

vertical angle is due to a destructive interference dip in the sound pressure field without a barrier that gets smoothed over when the barrier is present. Ignoring this dip, the larger two barriers have no effectiveness at the aft 45 degree azimuth angle, though the smallest barrier seems to provide a 10 dB reduction of sound for vertical angles greater than 75 degrees.

To analyze the effectiveness at 200 Hz, a ¼ model was created. This model encompasses the forward three rows of the air gun array (see Figure 3), and assumes the array is symmetrical in the fore/aft direction. This simplification was necessary in order to be able to acquire results at this frequency. The effectiveness of the three barriers is provided in Figure 25. In this case the longer barrier clearly provides more attenuation than the shorter barriers both laterally and at a 45 degree azimuth angle, particularly at the higher vertical angles. As the barrier is made smaller the effectiveness is reduced. It is interesting to note that the effectiveness is greater at the 45 degree azimuth angle than it is in the lateral direction.

These results indicate that longer barriers will be more effective at some frequencies, though short barriers, even barriers that are shorter than the air gun array, could provide increased attenuation at some frequencies. However, after comparing Figures 23 and 24 it can be said that a longer barrier will likely provide an overall increased performance. This is good because it would be difficult to make a bubble curtain with sharply defined vertical forward and aft edges, particularly when the array and bubble curtain is moving. Rather, it is easier to make a long bubble curtain relative to the air gun array size. However, the above result may be useful if a foam material is used for the barrier instead of air bubbles (see Section 3).

The results of the 3-D models also show that because the air gun array output is biased towards the forward end the barrier effectiveness is also biased for forward azimuth angles. Aft azimuth angles do not appear to perform as well. Although not shown here, the directivity in the longitudinal direction is essentially unchanged for any barrier, and thus the effectiveness of the barrier will drop off at some azimuth angle. The specific angle where this occurs will be dependent on the specific air gun array.

2.4 Conclusions – Bubbler Barrier

It is clear that some attenuation of laterally propagating sound from an air gun array can be achieved through the use of a longitudinally oriented air bubble curtain. For the modeled array, sound level reductions at frequencies of 100 Hz and above are on the order of 5-25+ dB for large vertical angles (i.e. closer to the water surface) where receivers are located on the side of the air gun array ('lateral' or 'transverse' direction). For air gun arrays that are biased at the forward end (i.e. larger air guns are placed at the front of the array) the barrier effectiveness will be greater at forward azimuth angles and less at aft azimuth angles. The barriers do not significantly change the radiation pattern on centerline. Barrier length in the forward/aft direction should generally be made as long as possible or practical to maximize effectiveness.

For the specific air gun array modeled here, attenuations were seen to begin at roughly 50 - 70 degrees relative to the vertical axis, depending on frequency. The angle where effectiveness begins will depend on the barrier depth and distance from centerline. Barriers that are very close to the air gun array show the best performance, significantly so even when compared to a barrier that is moved only a few meters away. Deep barriers will have better performance, though there

appears to be diminishing returns past a certain depth (12 meters for the array modeled here). The angles of effectiveness will also depend on the specific air gun array characteristics, including geometry, relative size of the air guns, and depth in the water.

The air content should be as high as is practical, with 10% air by volume being a good minimum design. Barrier thickness was not seen to be a dominant factor in performance for practical sizes.

It is important to note that increases in sound level have been noted for some frequencies and angles as a result of the use of a bubble curtain. This amplification appears to be generally limited to angles closer to vertical, though the specific angle and amount of amplification will depend on the specific frequency and barrier/air gun array characteristics. For example, the baseline barrier modeled here showed an approximate 8 dB increase in sound between the vertical angles of 54 and 67 degrees (2-D model). Amplifications as high as 20 dB have been noted for some of the modeled barriers. These amplifications occur at certain angles because the sound radiation from the air gun array *without the barrier* is reduced when there is destructive interference between the array elements and the water surface. When the barrier is added the sound level may in fact be relatively smooth at these frequencies, but when compared to the sound level without the barrier there is a relative amplification.

It cannot be generally said that higher frequencies are attenuated more than low frequencies because of the specific geometry and pressure release surfaces that exist⁵. For the array modeled here, the baseline barrier produced 27 dB of reduction at 400 Hz for a vertical angle of 75 degrees while at 600 Hz only 6 dB of reduction was seen. These effects were nearly reversed when the barrier was moved closer to the array. Again, actual barrier attenuations will be dependent on the specifics of the array and barrier.

Another important result is the possible reduction in sound of low frequencies (<100 Hz) directly below the array. While most frequencies below 100 Hz were largely unaffected by the barrier, some configurations showed reductions of sound as high as 12 dB directly below the array at specific frequencies (e.g. 30 Hz). This is an important result as these frequencies are useful in identifying geological features beneath the sea floor.

If the barrier is used in shallow water (~20-30 meters) then the reflections off the sea floor will act to reduce the effectiveness of the barrier. Using a 'perfectly rigid' approximation for the sea floor all frequencies were seen to have significant reductions in effectiveness. No reduction in sound was seen at some frequencies that otherwise show some sound reduction in deep water. For realistic sea floors it is expected that the reduction in performance would not be quite this dramatic, though the results will depend on the specific makeup of the sea floor and the amount of sound that is absorbed.

Given the fact that the performance of any barrier is strongly dependent on the air gun array configuration, it is suggested that some modeling be performed to help optimize the location and size of the barrier for maximum effectiveness. This modeling will also help to identify and

⁵ This is generally true for hard in-air barriers.

minimize amplification of unwanted sound at large vertical angles as well as identifying any possible reduction of sound below 100 Hz under the array.

3.0 LOW IMPEDANCE BARRIER MATERIALS

While bubble curtains have been shown in the literature to be effective at blocking sound propagation, they can sometimes be difficult to work with [1]. Set-up is critical, and includes properly locating air hoses and getting the air pressure and flow correct, among other factors. Bubble curtains are also susceptible to currents; if the bubble curtain is not contiguous then reductions in performance can result. Marine fouling can also be an issue, clogging the holes in the hoses and reducing performance. While it is certainly possible to successfully use air bubble curtains in practice, a more consistent alternative may be desirable.

Reference [6] shows that closed cell foam attached to the interior of a steel pipe can be used as an effective barrier against pile driving noise. The sound level reduction was seen to be similar to if not better than an air bubble curtain. Reference [7] indicates that large attenuations can be gained in similar applications through the use of closed cell foam alone (no steel backing). It is believed that the underwater noise attenuation that occurs is a result of the fact that the foam has integrated air (or gas) pockets. As is the case at the surface of the water, the water-air interface poses a large impedance mismatch, causing a reflection. To a first order approximation, the closed cell foam acts to put air into the water and keep it in place, thus becoming as an acoustic barrier.

It can be argued that the material lattice that makes up the foam will provide some impact on the acoustic reflectivity or transmissibility of the foam as a whole. To investigate this it is possible to determine the specific acoustic impedance of the foam and compare it to the water to see if there will be a sufficient impedance mismatch. As noted before, air is a pressure release material relative to water. The specific acoustic impedance of air (density * speed of sound) is 415 rayls, and the specific acoustic impedance of water is 1.5e6 rayls, or 3500 times greater. It was shown in Section 2 that injecting 10% air by volume into water creates a fluid with an impedance that is 33 times lower than water, and this still approximates a pressure release surface. Thus, in order for a foam material to work in this application, it should have an impedance that is at least 30 times less than water.

Neoprene and nitrile foams have been used in several applications as an underwater acoustic decoupling materials on vessels [1, 8]. Rubatex Corporation (www.rubatex.com) manufactures a nitrile foam R-437 with a density of 160-352 kg/m³, tensile strength of 1200 kPa, and low water absorption. The pressure required to compress this material to 25% of its thickness is approximately 76 kPa. After using this figure to calculate an approximate Young's modulus, the compressive wave speed in the material is calculated to be on the order of 20 m/s. This yields a specific acoustic impedance of 5000 rayls, which is 300 times less than water. As a result, this material appears to be appropriate for use as an underwater sound barrier.

Other foams such as neoprene, EPDM, and hybrids also appear to be appropriate for this purpose. These foams are all relatively limp and are capable of being rolled and stored on a vessel. However they may also create increased drag if placed in the ocean due to oscillating lateral motion similar to a flag in wind. They will also need to be ballasted down to maintain the

appropriate depth. A metal backing plate or other supporting structure may be desirable here, acting both as ballast and structural support.

A hard or quasi-rigid foam, as used in References [6, 7], may be another option that would be more likely to hold its shape in the water, thereby reducing drag. Reference [9] presents material properties of some polyurethane foams with densities ranging from 120 to 320 kg/m³. The compressive Young's modulus is shown to increase with increasing density. The highest density foam has a specific acoustic impedance for compressive waves that is only 6 times less than water, while the lowest density foam is 30 times less than water. However, bending waves will likely be most important here, and the calculated specific acoustic impedance using the bending wave speed is much less than that of water. Therefore, from an acoustic perspective, polyurethane closed cell hard foams should also be appropriate for this application, though lower density foams may provide a slight acoustic advantage. Other rigid foams may be appropriate as well, though their material properties should be analyzed to determine their specific acoustic impedance. From a non-acoustic perspective, hard foams may be more difficult to deploy and retrieve than soft foams.

It was shown in Section 2 that the barrier thickness, when varied between 1 and 12 inches, did not significantly influence effectiveness. However, in the limit of vanishing thickness the effectiveness would go to zero. Therefore at some thickness there will be a reduction in performance. The model assumes that the overall shape of the barrier does not change. In water, the particle motions resulting from sound levels expected from an air gun are much less than 1 mm. However, in a material with an acoustic impedance 30 times less than water the particle motions can be more significant. At a level of 210 dB re 1μPa, a 30 Hz wave will cause particle motions on the order of 3 mm, and at 10 Hz the motion will be 10 mm. It is reasonable to believe that the thickness of the barrier should be much more than the expected particle motion within the barrier. For the above case, a minimum thickness of 25 mm (1 inch) should be sufficient, though physical testing is recommended.

It is noted that in both Reference [6, 7] the thickness of the (hard) closed cell foam was 2-16 inches. A thicker barrier should not compromise acoustical effectiveness, though non-acoustic factors such as space, weight, and costs would be affected. Stiffness is also a consideration, as noted above.

4.0 PARABOLIC REFLECTOR

4.1 Background

Parabolic reflectors are commonly employed to focus waves of various types at a central point. Parabolic reflectors are used in various applications, such as with microphones on the side of a football field where the broadcasting network is trying to hear the grunts of the players on the field. The reflector takes the otherwise omni-directional microphone and creates a highly directional receiver. If a source were placed at the apex of the reflector instead of a microphone then the radiation would also be highly directive.

It may be possible to apply this concept to air gun arrays as well. A concept sketch is provided in Figure 26. In this design a barrier is located above the air gun source in the shape of a parabola with the intention of focusing sound in the downward direction. The sketch is a lateral

cross section, and shows a single row of sources (air guns). Because there is only a single row of air guns, the array could be made longer than in a typical air gun array while retaining the same number of air guns. This would increase longitudinal directivity, while the reflector would increase lateral directivity.

Initially the barrier is assumed here to be an air bubble curtain, similar to what was used in Section 2 of this report. Based on the results of Section 2, it is clear that the air bubble curtain would approximate a pressure release surface, which creates a reflection with inverted phase, as long as the air content is greater than 10% by volume⁶. A reflector made from a solid material is considered here as well.

4.2 Modeling

A 2-D finite element model was created in ComsolTM to model the air gun array and reflector. The model and analysis approach is similar to the 2-D models built to model the air bubble curtain described in Section 2, with the major differences being the modeling of the reflector and the different array geometry. Because the reflector is oriented in the lateral direction, it is assumed that the entire area above the reflector is an air-water mix. A screen capture of one model is provided in Figure 27. Note that in practice in order to achieve a consistent reflector shape over the entire air gun array multiple hoses will be needed along the length of the array. Both deep and shallow water applications were modeled here.

The air gun array was varied between 3 and 6 meter depths. The reflector was created so that the air guns were located at the focus of the parabola, using the following equation:

$$Depth = \frac{1}{4a} x^2$$

where a is the distance between the array and the water surface and x is the distance from centerline. The reflector was made to coincide with the water surface at $x = 0$. This means that the width of the reflector was always $4a$ at the depth of the array (dimension b in Figure 26). The reflector size was varied by changing the largest distance from centerline. For the 3 meter deep array, the reflector was varied between $x_{max} = 9 - 15$ meters (18 - 30 meter total width), corresponding to reflector depths of 6.75 - 18.75 meters, respectively. For the 6 meter depth array the reflector shape was wider and shallower. The size was varied between $x_{max} = 12-20$ meters, corresponding to reflector depths of 6 and 16.7 meters, respectively.

The air bubble reflector was assumed to have 10% air by volume, yielding a density of 900 kg/m³ and a 45 m/s speed of sound. A pressure release surface was also modeled separately for comparison purposes (water was assumed to exist directly over the reflector in this case).

⁶ Creating an acoustically hard surface in water is difficult and may not be practical for this application. For example, if a metal sheet were used instead of an air bubble layer, the impedance would be controlled by the bending wave speed of the plate. This speed is very low at the frequencies of interest, and the characteristic impedance would not be sufficiently greater than the impedance of water.

4.3 Results

As was noted in Section 2, the array directivity without a reflector must be established in order to determine the effectiveness of the reflector. A plot of the normalized output of the 3 meter deep array vs. vertical angle is provided in Figure 28. It is noted that the directivity of this array is slightly more uniform than the array modeled in Section 2 because there is only a single line of air guns. However, it is important to note the large dips in output at certain angles for higher frequencies – these dips will create apparent increases in sound when the reflector is used, as discussed in Section 2.

Figures 29, 30, and 31 present the effectiveness of three reflector configurations for the 3 meter deep array. In comparing these figures it is clear that a larger reflector will be more effective at reducing lateral propagation than a smaller reflector. For the largest reflector, reductions in sound of 30-40 dB are seen at 400-600 Hz at vertical angles above 70 degrees; however at 100 and 200 Hz the reductions in sound are only on the order of 0-5 dB for these angles. For the ‘medium’ sized reflector the reduction in sound is more consistent, with 20+ dB reductions seen for 200-600 Hz at vertical angles greater than 70 degrees. Even the small reflector shows 10-15 dB reductions at frequencies above 100 Hz for vertical angles greater than 70 degrees. Furthermore, the vertical angle where reductions begin is seen to be approximately 30 degrees for the large reflector and 40 degrees for the medium and small reflectors.

Directly below the array, nearly all frequencies have a 0-10 dB increase in sound, which is advantageous to seismic exploration. The exceptions here are at 5 and 30 Hz, where 0-17 dB reductions are seen depending on the specific reflector size.

Similar results are seen for the 6 meter deep array, though in general the reductions in sound are not as great. Figure 32 shows the effectiveness of a reflector that is 24 meters wide but only 6 meters deep (depth being controlled by the equation in Section 4.2). Because the reflector does not extend below the array the effectiveness is minimal. A larger reflector will have greater effectiveness, but the width will become very large before an appreciable depth is achieved (a 12 meter deep reflector would require a total width of 44 meters).

Figure 33 shows the effectiveness of the ‘medium’ sized reflector used with the 3 meter deep array in water that is 30 meters deep. As was discussed in Section 2, the sea floor was assumed to be a hard reflecting surface. Similar to what was shown in Section 2, the ability of the reflector to reduce lateral sound levels is significantly reduced. In this case the sound is actually amplified by roughly 10 dB at 200 and 600 Hz.

Lastly, if the reflector is modeled as a simple pressure release surface the results are similar to those seen for the air bubble reflector. Figure 34 provides the effectiveness of the medium size reflector applied to a 3 meter deep air gun array when modeled with a pressure release surface. These results are seen to be similar, though not identical, to those of Figure 30. The pressure release surface could be considered to be a rough model of a solid material containing air pockets, as discussed in Section 3. Thus, it can be said that instead of an air bubble reflector, a solid material could be used to create the reflector.

4.4 Conclusions - Reflector

The parabolic reflector has a potential for large reductions in sound, particularly at vertical angles greater than 70 degrees. Compared to the effectiveness of the vertical barriers modeled in Section 2, the reflector appears to provide similar or greater reductions in sound over a larger vertical angle. The reflector is seen to provide an increase in output directly below the array of up to 10 dB for most frequencies, though the lowest frequencies (5, 30 Hz) can have reductions in sound of up to 17 dB. It is noted again that if the number of air guns used is held constant, a single line array can have greater directivity in the longitudinal direction (on centerline) than an array with 3 rows of guns, further improving the performance of this arrangement.

However, the size of the reflector may be a practical limitation, particularly for arrays positioned deeper in the water. If an air bubble curtain is used, the hoses used to create the air bubble curtain must be oriented laterally (transverse), and many rows of hoses must be used in order to maintain the parabolic shape over the entire array. This may prove difficult in practice. A solid material may be preferable in this case, and would also provide similarly large sound level reductions. Such a reflector would likely need to be assembled in sections to cover the entire length of the array. Possible candidate materials have been discussed in Section 3.

As was found for the vertical barriers of Section 2, the effectiveness in shallow water is significantly compromised as a result of bottom reflections. If the sea floor is absorptive then this reduction in performance may not be as dramatic.

REFERENCES

1. J. Spence et.al., "Review of Existing and Future Potential Treatments for Reducing Underwater Sound from Oil and Gas Industry Activities," NCE Report 07-001, December 31, 2007.
2. G. Costigan, P.B. Whalley, "Measurements of the speed of sound in air-water flows," *Chemical Engineering Journal* **66** (1997) 131-135.
3. E. Sixma and S. Stubbs, "Air Bubble Screen Noise Suppression Tests in Lake Maracaibo," Sociedad Venezolana de Ingenieros Geofisicos *Congreso Venezolano de Geofisica*, 1996.
4. L. Beranek, *Noise and Vibration Control*, McGraw Hill, New York, 1971.
5. B. Dragoset, "Introduction to Air Guns and Air-Gun Arrays," *The Leading Edge*, August 2000, pp.892-897.
6. J. Laughlin, "Underwater Sound Levels Associated with Driving Steel and Concrete Piles near the Mukilteo Ferry Terminal," Report for WSF Mukilteo Test Pile Project, March 2007.
7. K. Lucke, "Protecting Sensitive Ears Underwater from Impulsive Sounds," Presentation at the *Workshop and Review of Noise Reduction Technologies Capable of Reducing Underwater Acoustical Footprints*, Burlington MA, June 2007.
8. M.J. Coughlin et.al., "Design of a Hull Coating to Reduce Interior Propeller Cavitation-Induced Noise for the PGG 511 Class Patrol Gunboat," Bolt, Beranek, and Newman Technical Memorandum No. W473, April 1979 (not commercially available).
9. M. Thompson, I. McCarthy, and L. Lidgren, "Compressive and Shear Properties of Commercially Available Polyurethane Foams," *Transactions of the ASME*, Vol. 125, October 2003, pp.732-734.

FIGURE 1: Theoretical and Measured Sound Speed in Air-Water Mixture vs. Air Content [2]

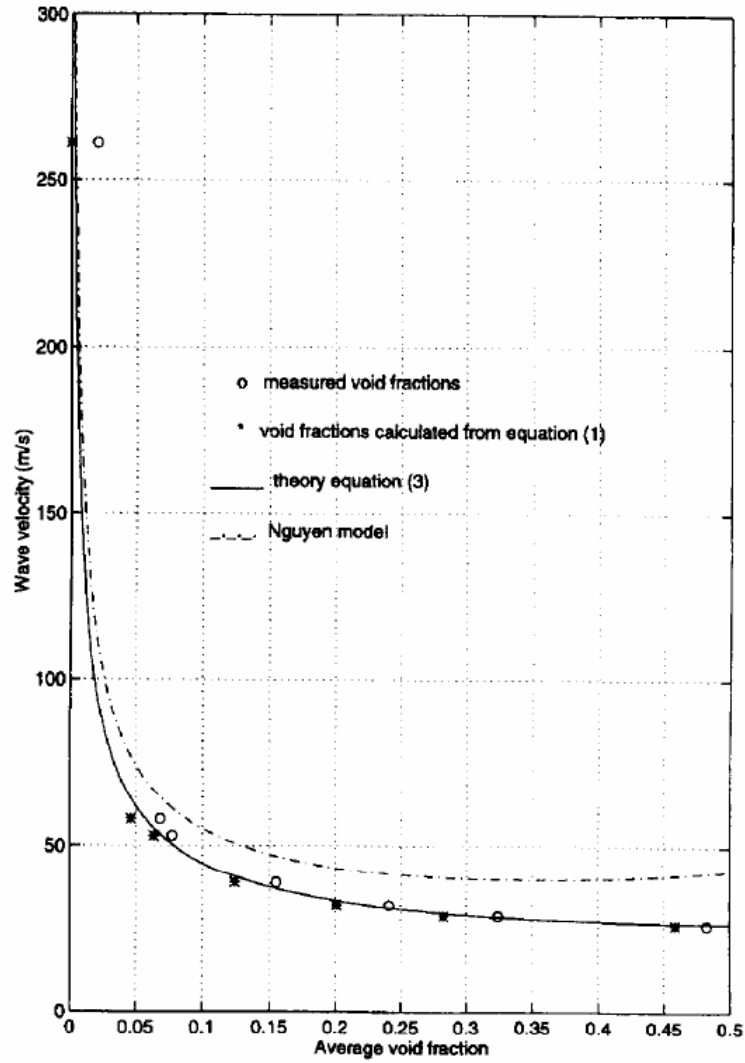
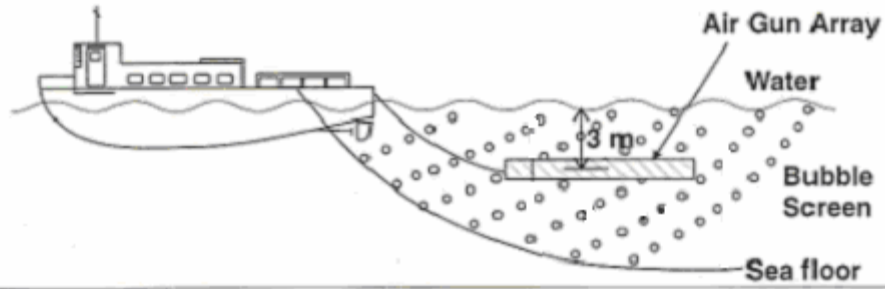
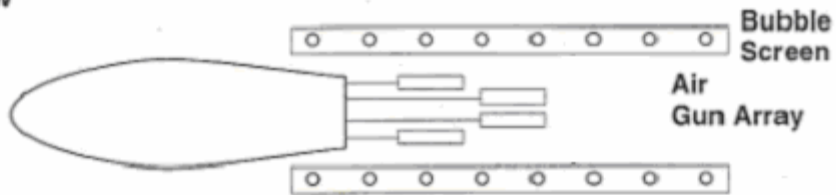


FIGURE 2: Underwater Air Curtain Barrier Concept [3]

Side view



Top view



Front view

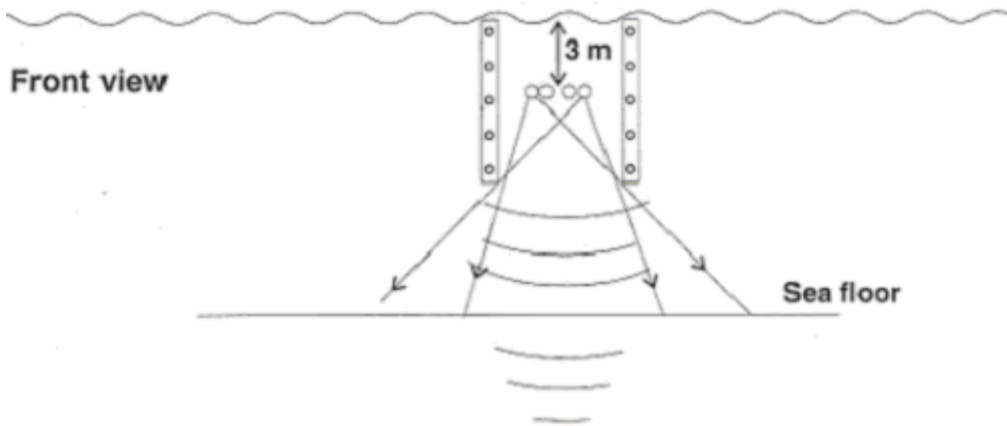


FIGURE 3: Example Array Design (from [5])

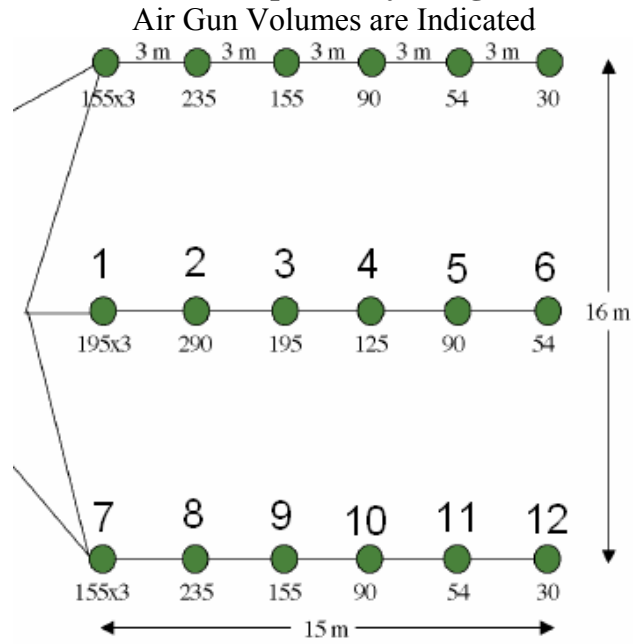


FIGURE 4: Example 2-D Deep Water Model

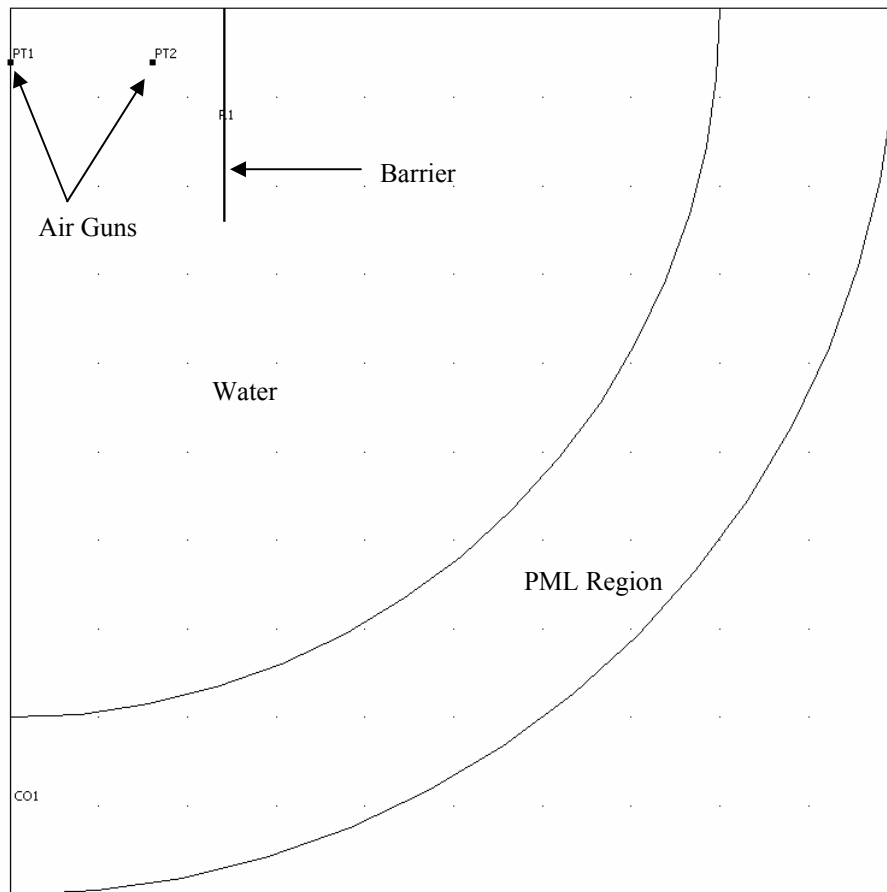


FIGURE 5: Example 2-D Shallow Water Model

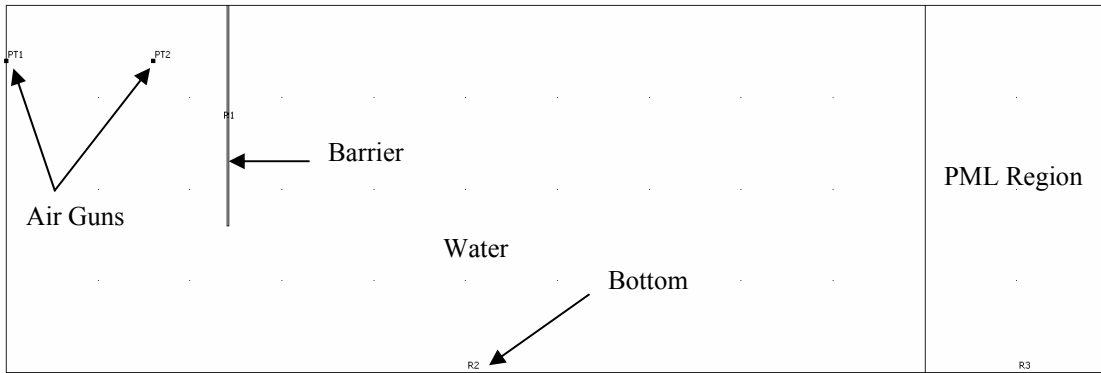


FIGURE 6: Example 3-D Deep Water Model

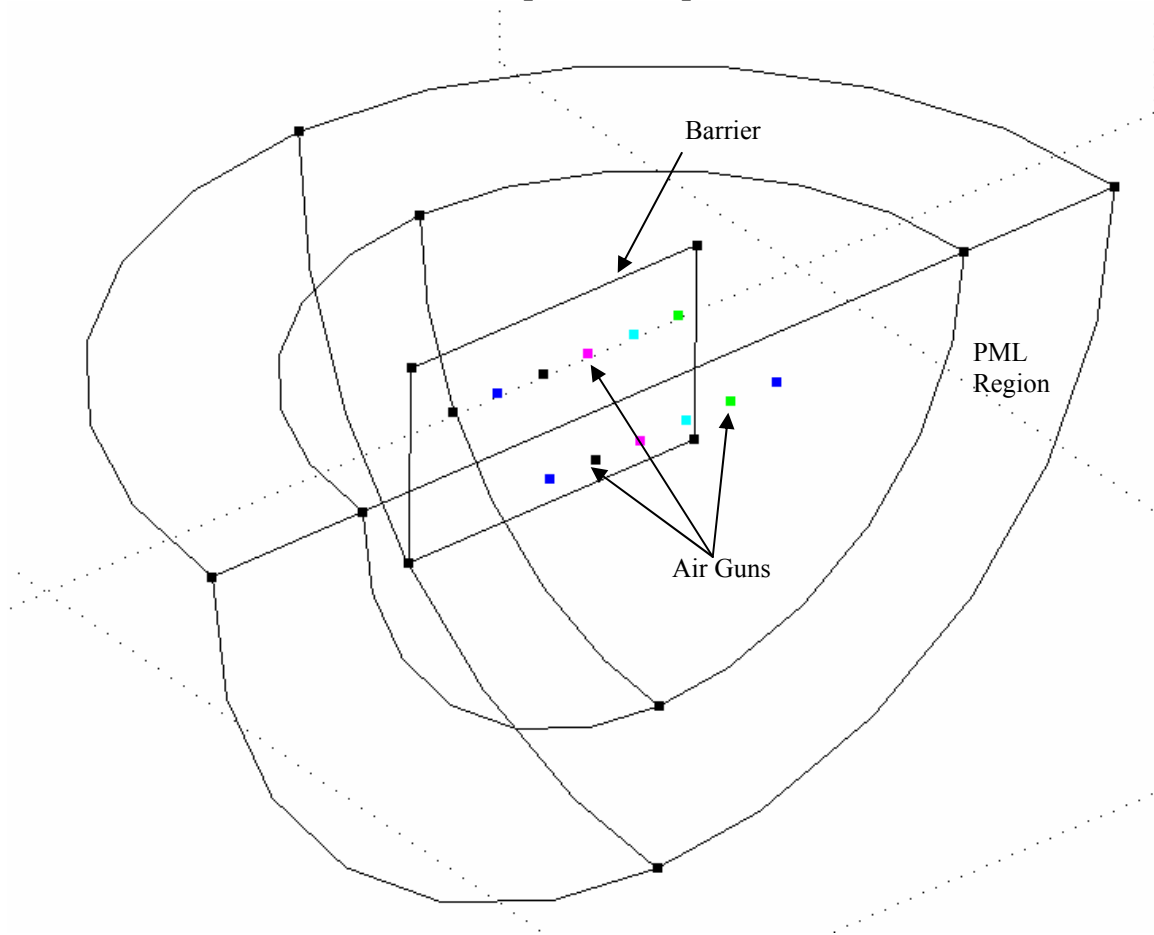


FIGURE 7: Directivity for 2-D Deep Water Model, No Barrier

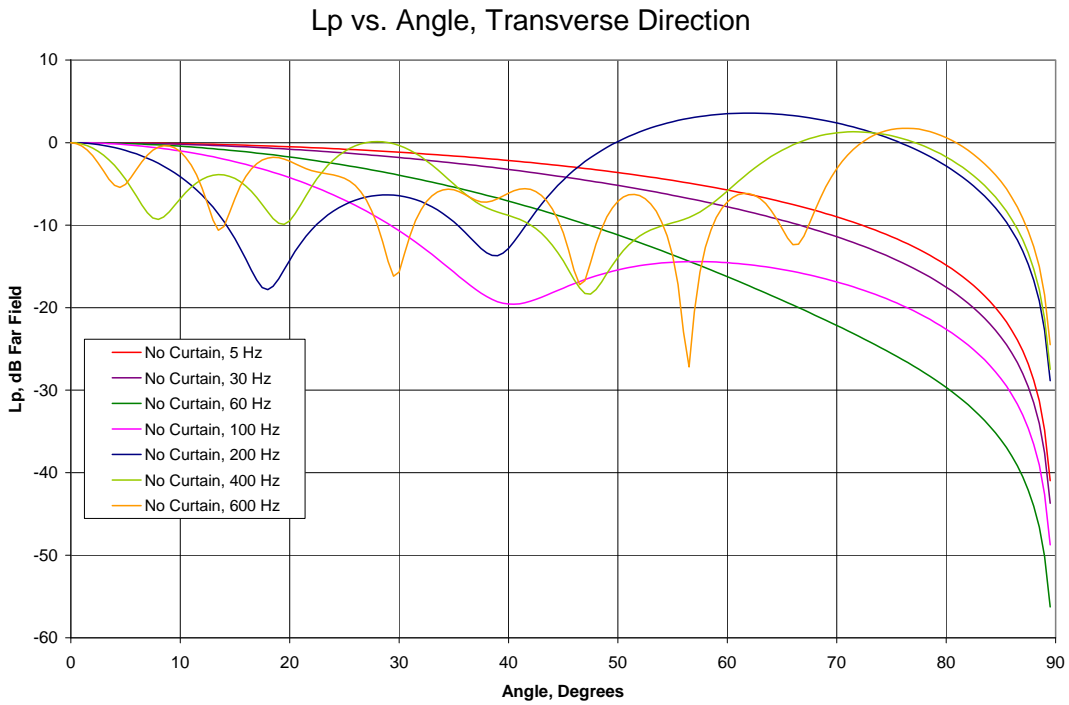


FIGURE 8: Barrier Effect for 2-D Deep Water Model, Baseline Barrier

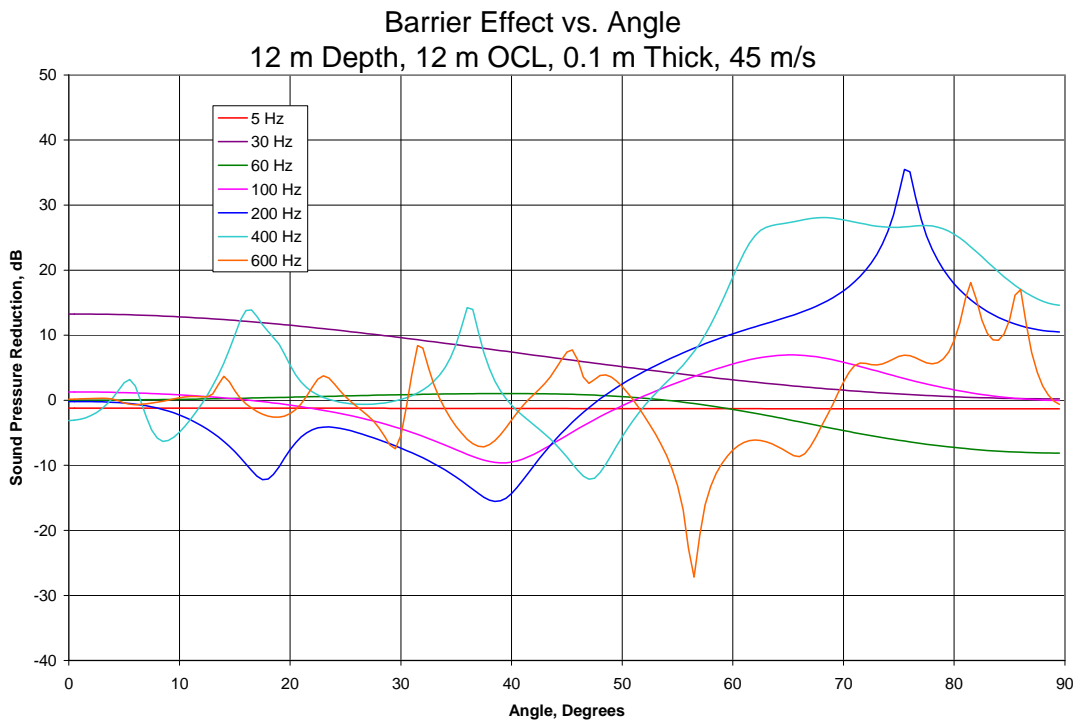


FIGURE 9: L_p in dB, 2-D Deep Water Model, Baseline Barrier, 30 Hz
Note absolute level is arbitrary

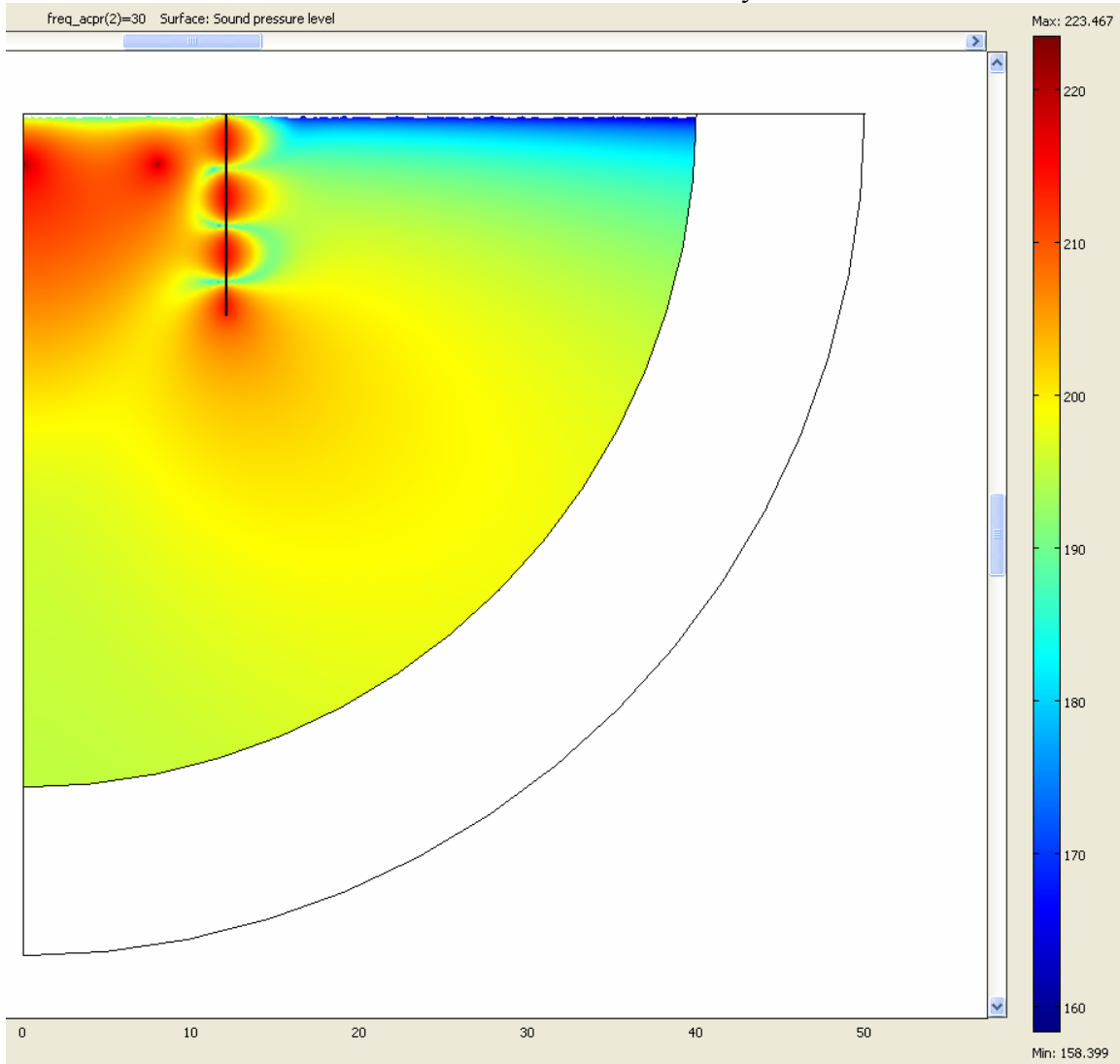


FIGURE 10a: Lp in dB, 2-D Deep Water Model, Baseline Barrier, 600 Hz
Note absolute level is arbitrary

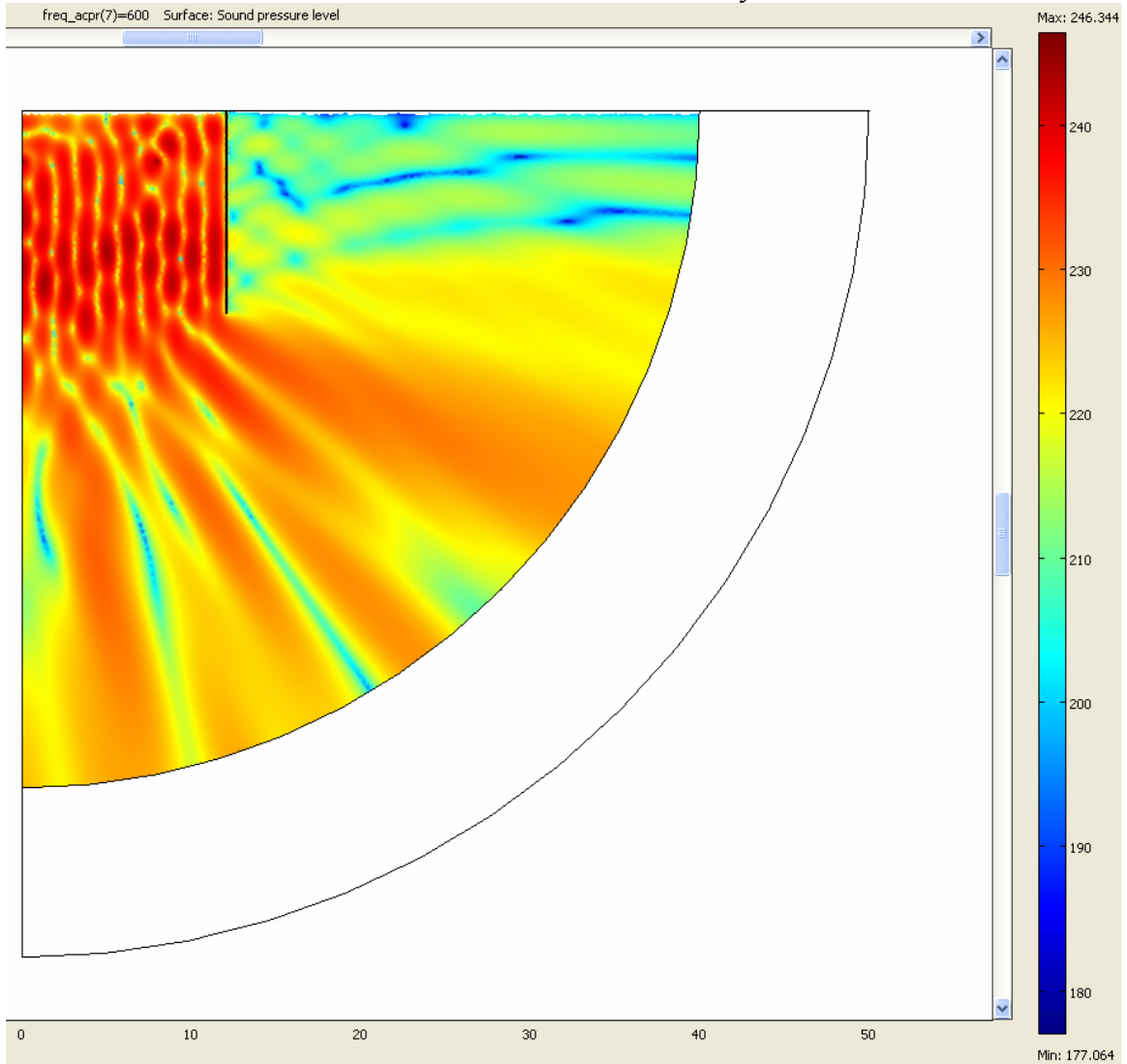


FIGURE 10b: Comparison of Lp for Baseline Barrier vs. No Barrier, 600 Hz, 2-D Deep Water Model

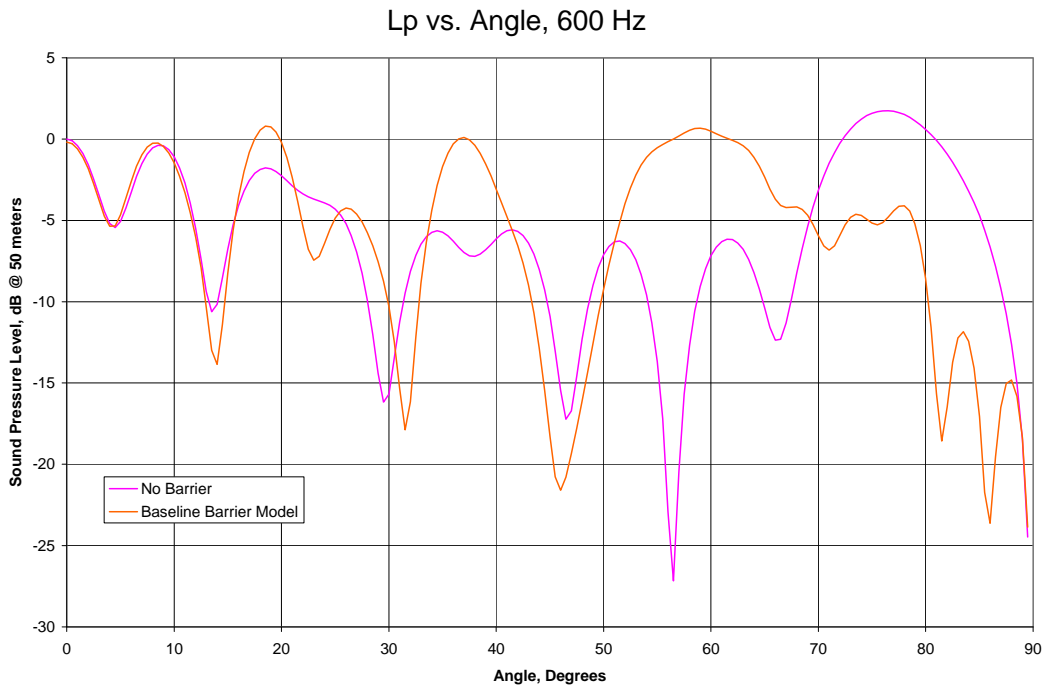


FIGURE 11: Barrier Effect for 2-D Deep Water Model, Deep Barrier

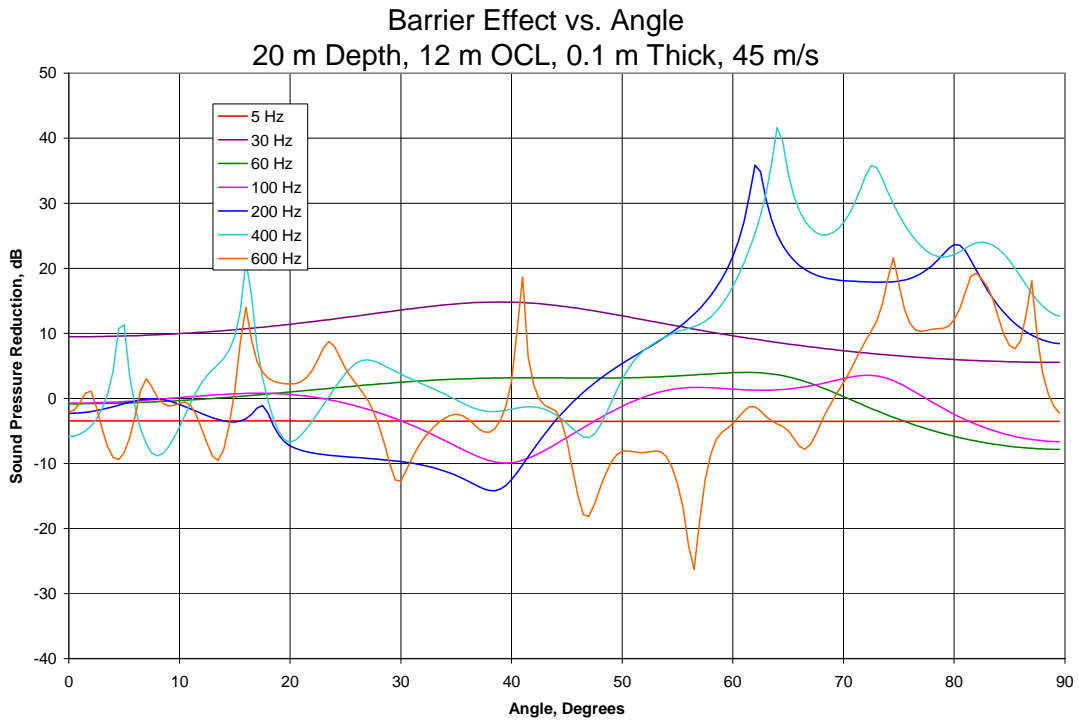


FIGURE 12: Barrier Effect for 2-D Deep Water Model, Shallow Barrier

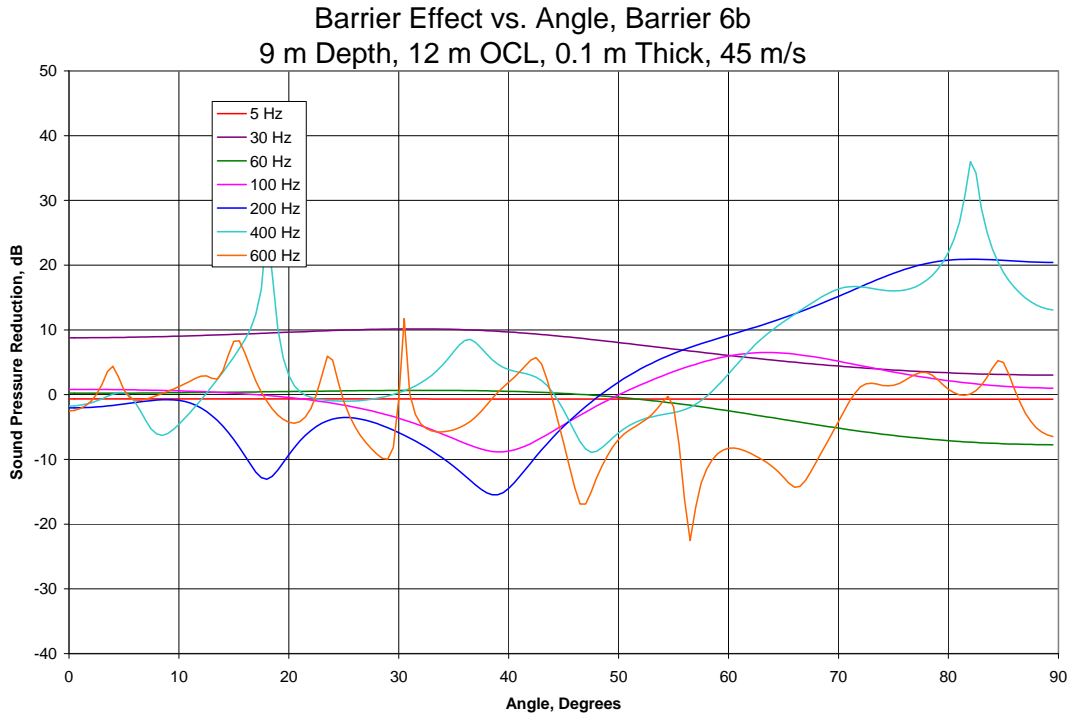


FIGURE 13: Barrier Effect for 2-D Deep Water Model, Close Barrier

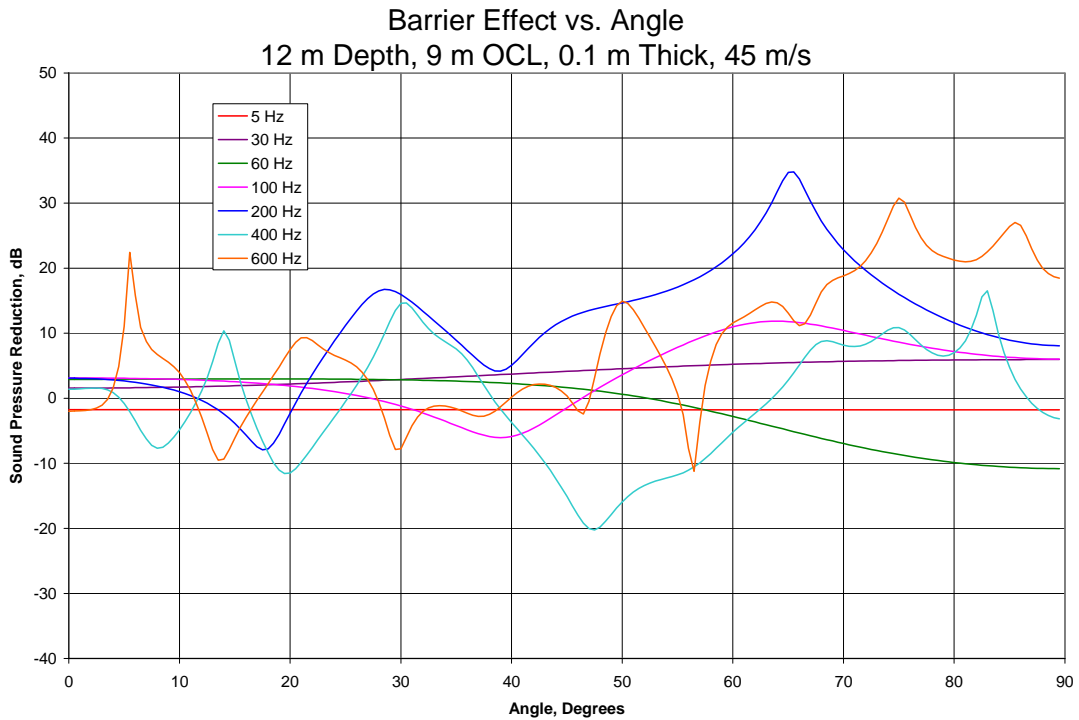


FIGURE 14: Barrier Effect for 2-D Deep Water Model, Far Barrier

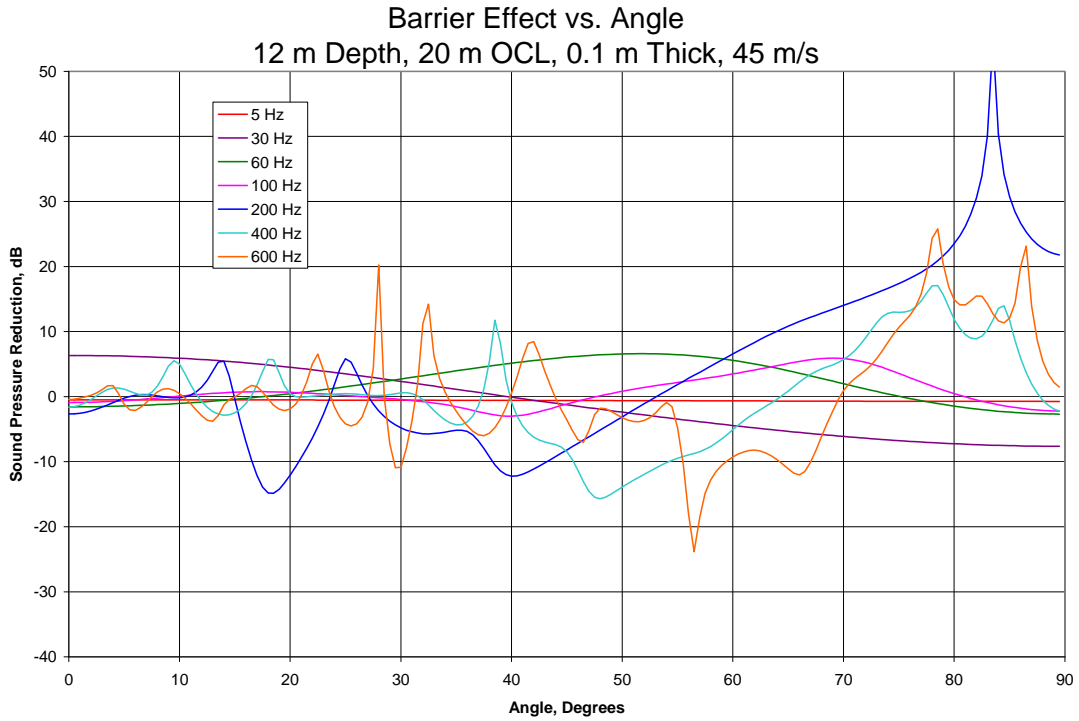


FIGURE 15: Barrier Effect for 2-D Deep Water Model, Low Saturation Barrier

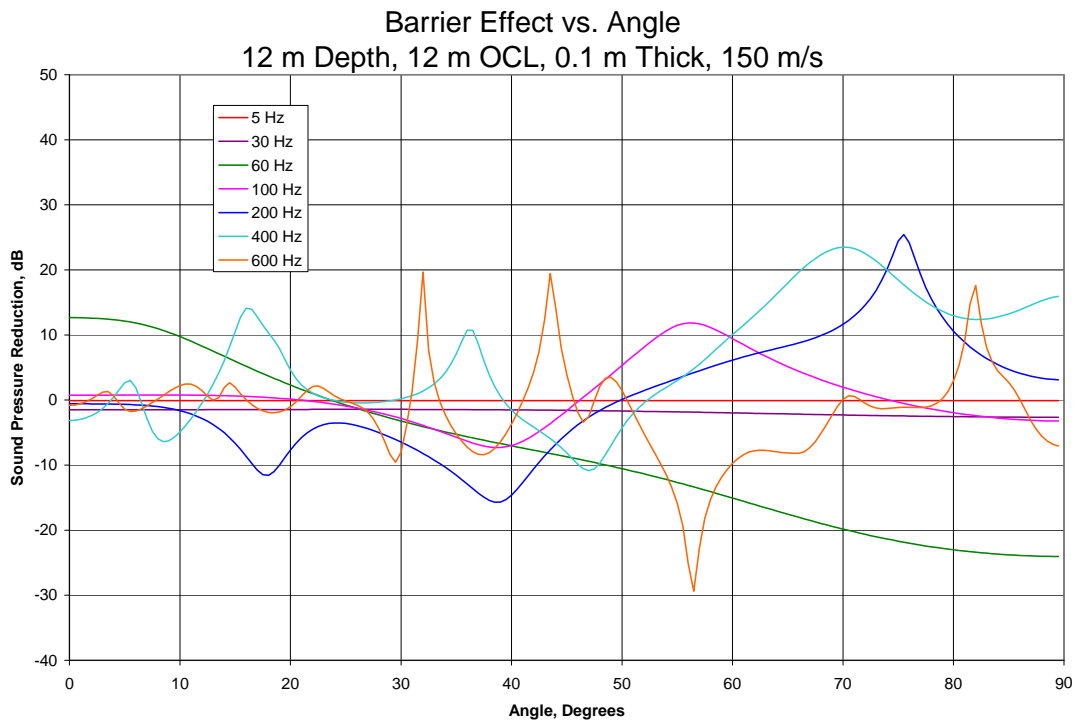


FIGURE 16: Barrier Effect for 2-D Deep Water Model, Thick Barrier

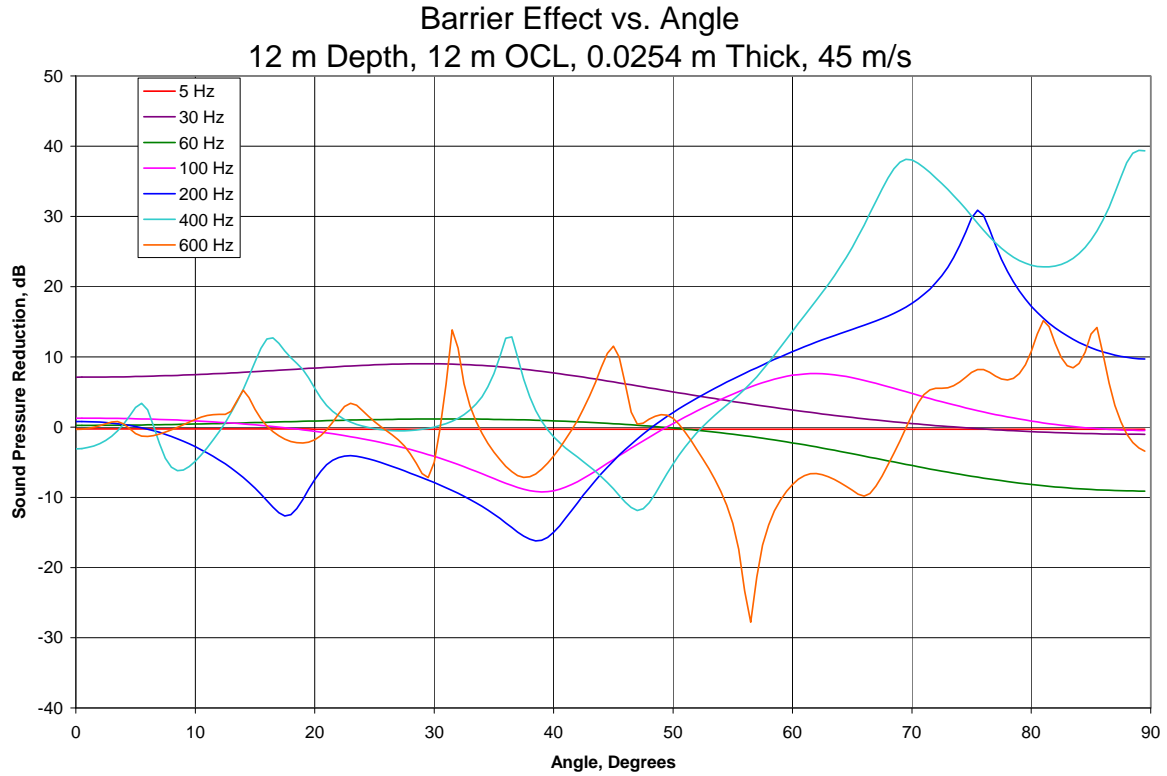


FIGURE 17: Barrier Effect for 2-D Deep Water Model, Optimized

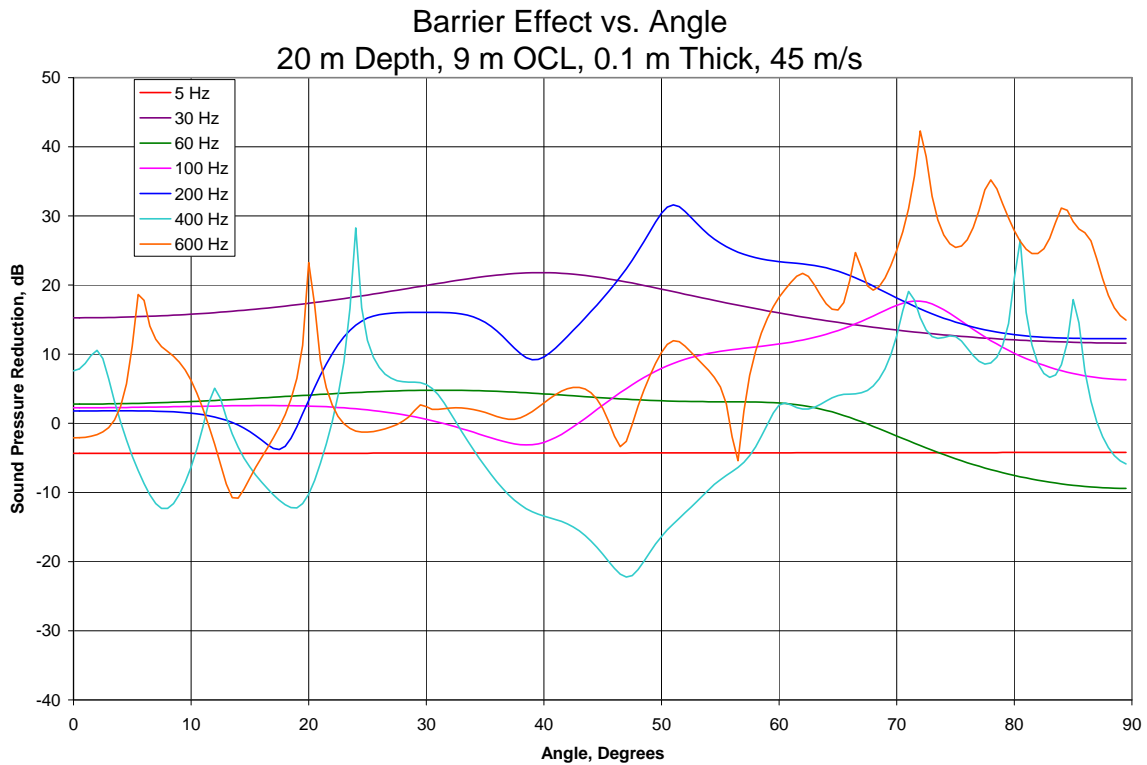


FIGURE 18: Sound Level in dB, 2-D Shallow Water (30 meter) Model, No Barrier, 600 Hz

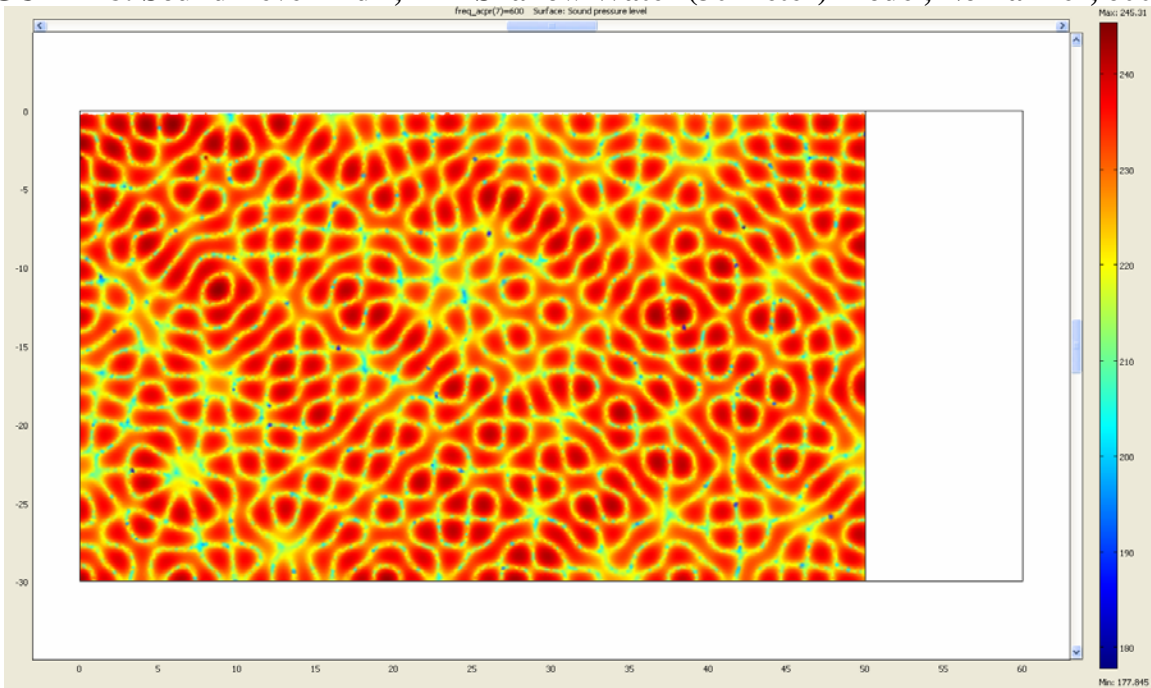


FIGURE 19: Barrier Effect for 2-D Shallow Water Model, 20 meter Depth

Barrier Effect vs. Depth, Baseline Barrier,
20 m Depth w/ Hard Bottom

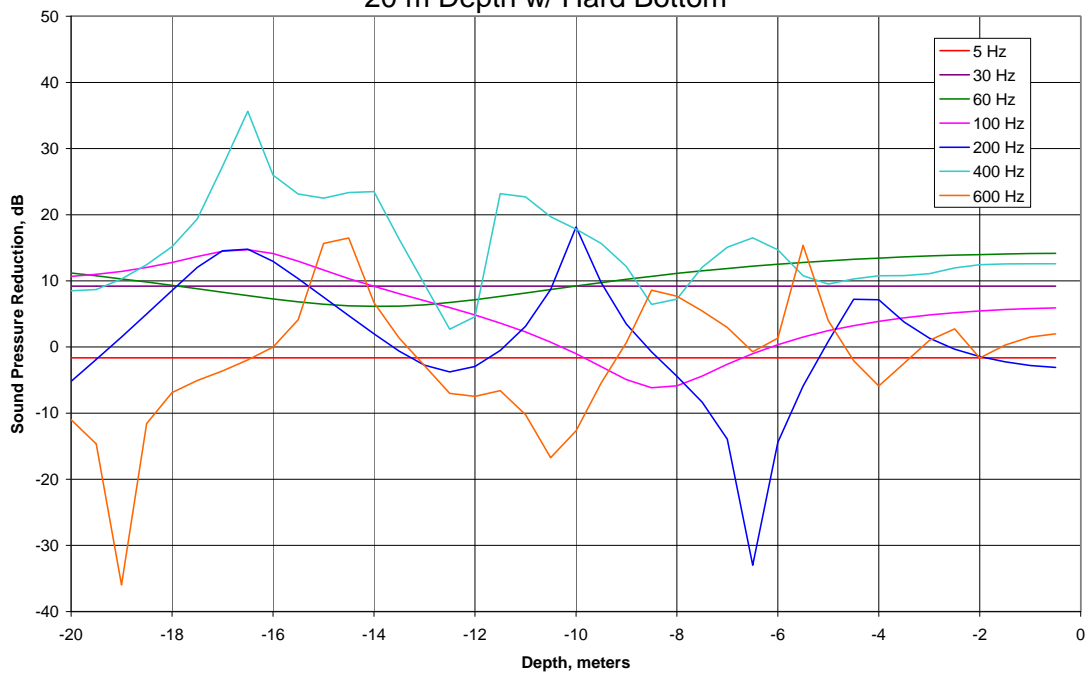


FIGURE 20: Barrier Effect for 2-D Shallow Water Model, 30 meter Depth
 Barrier Effect vs. Depth, Baseline Barrier,
 30 m Depth w/ Hard Bottom

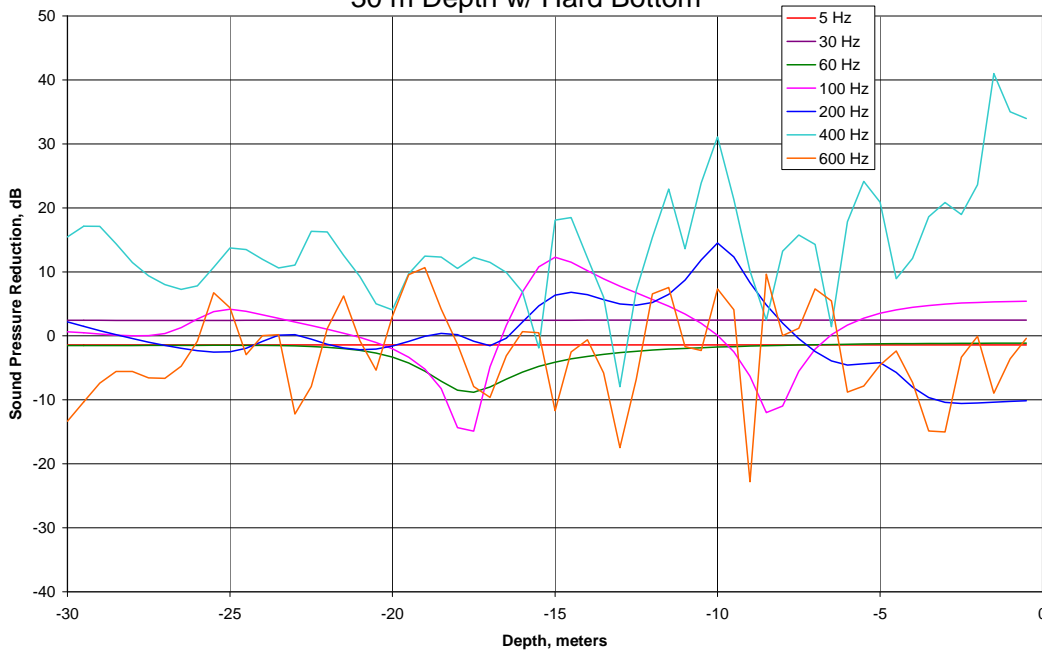


FIGURE 21: 2-D Model Results for Baseline Barrier vs. Pressure Release Surface

Comparison of Pressure Release vs. Explicit Model of Barrier

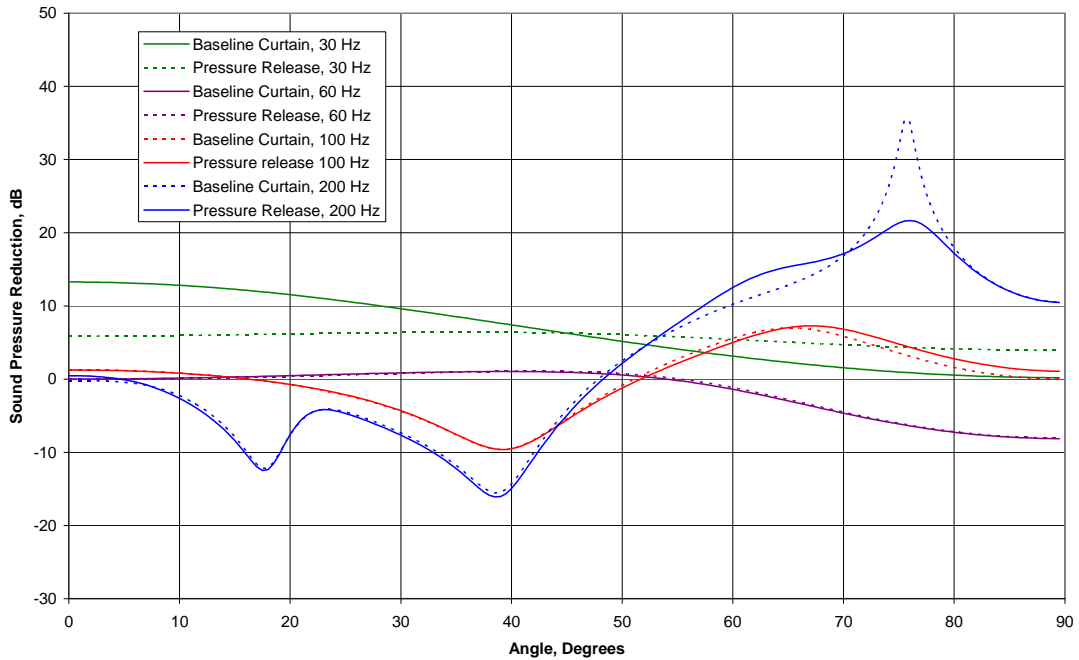


FIGURE 22: Comparison of 3-D vs. 2-D Model Results

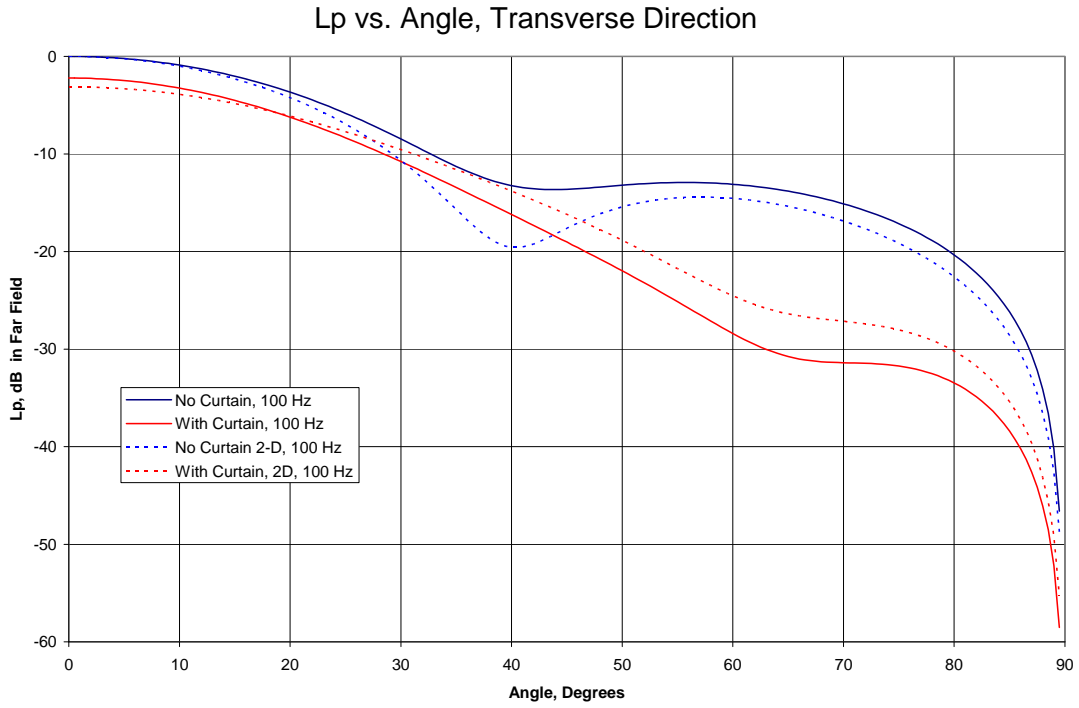


FIGURE 23: Plot of Results Extraction Locations

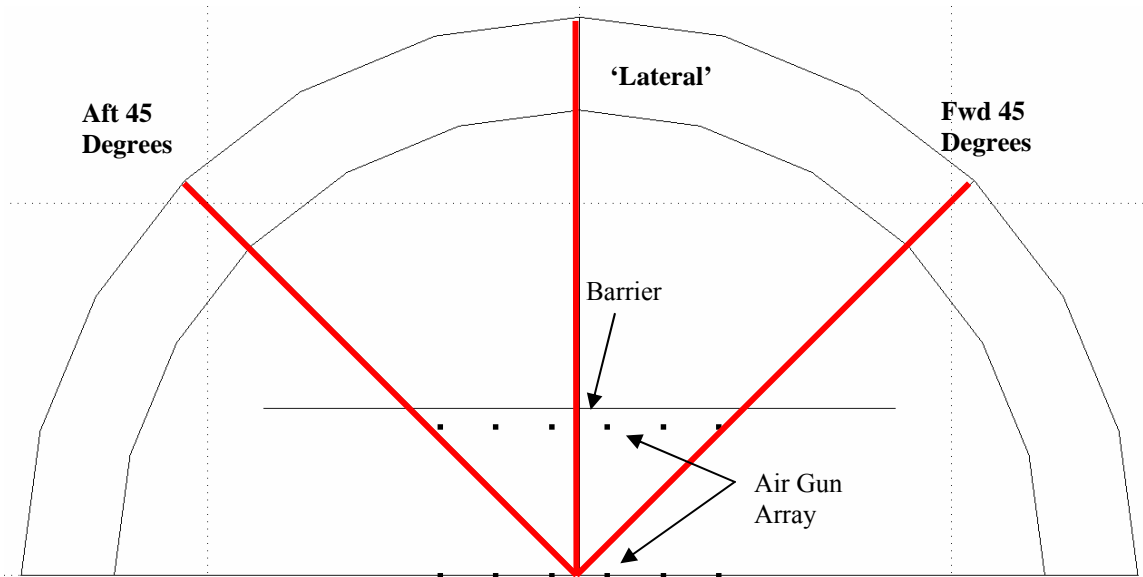


FIGURE 24: Barrier Effect for 3-D Model, 100 Hz

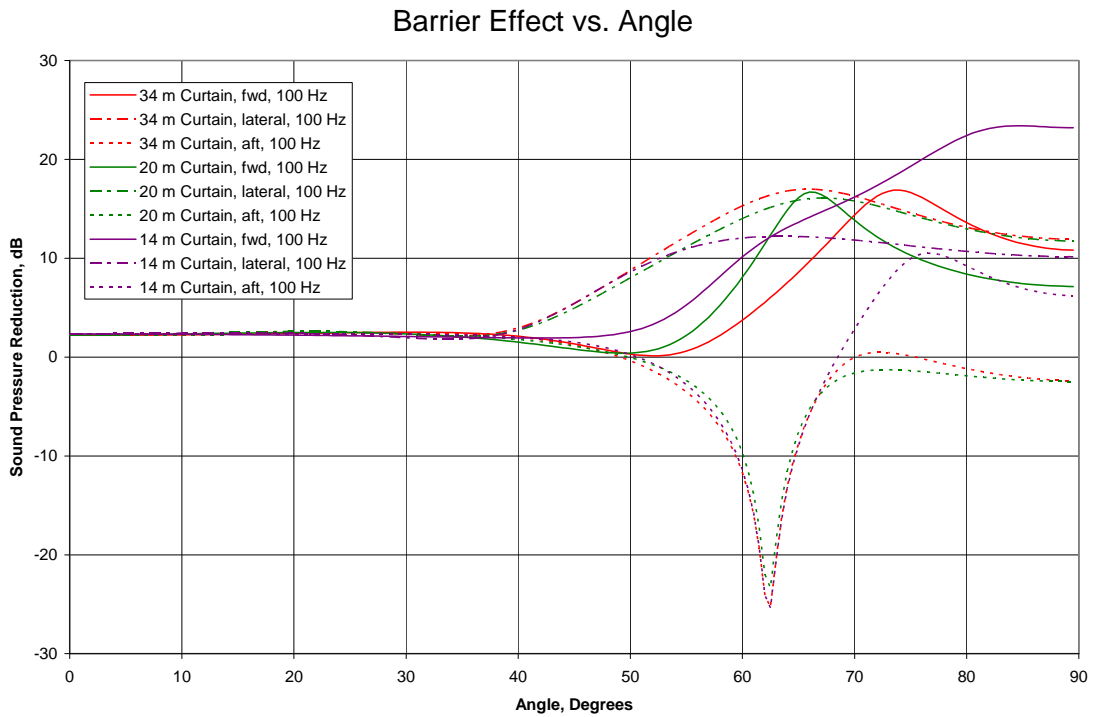


FIGURE 25: Barrier Effect for 3-D Model, 200 Hz

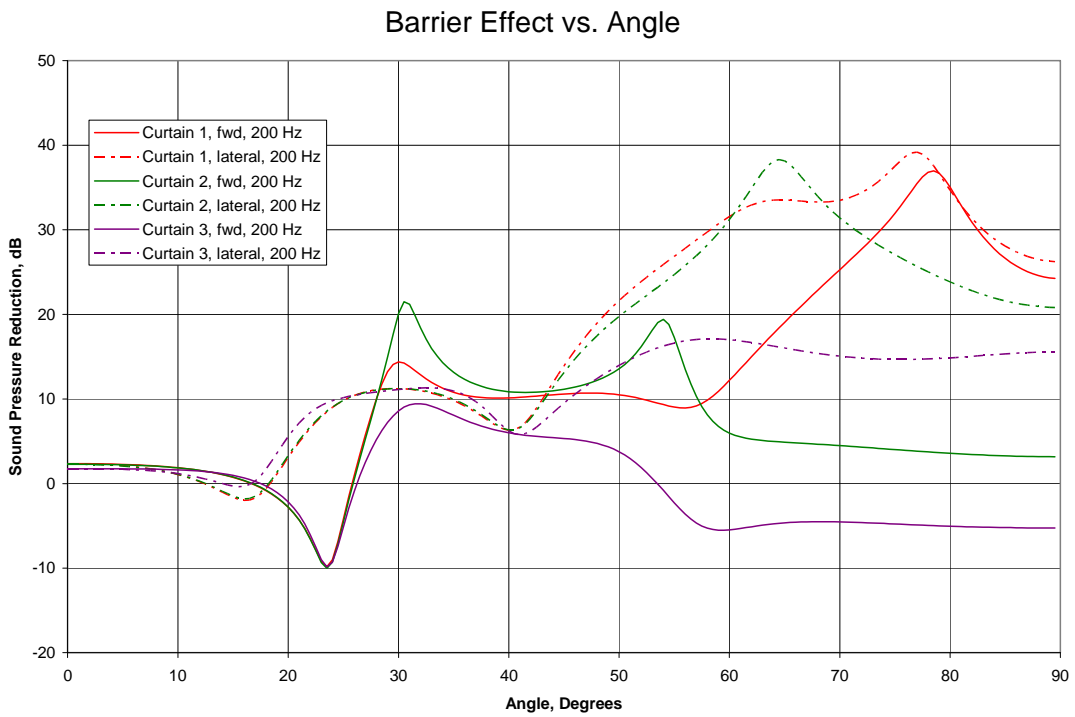


FIGURE 26: Concept Sketch of Parabolic Reflector

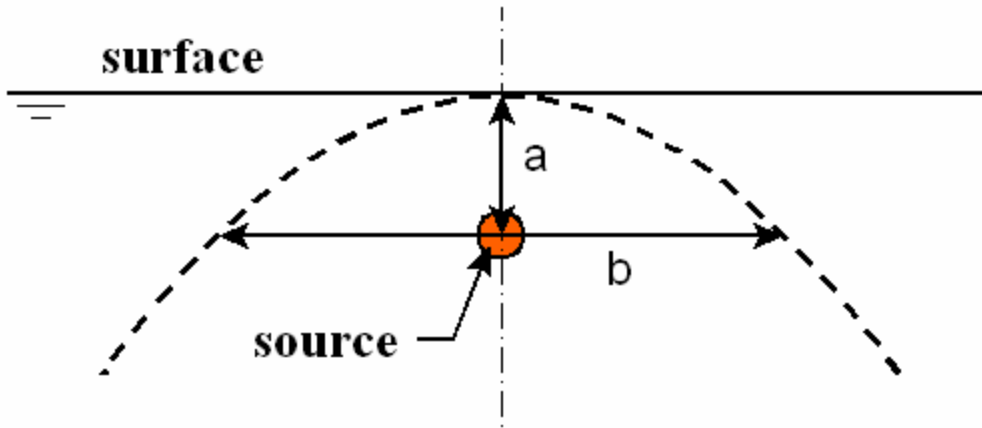


FIGURE 27: Example Parabolic Reflector Model

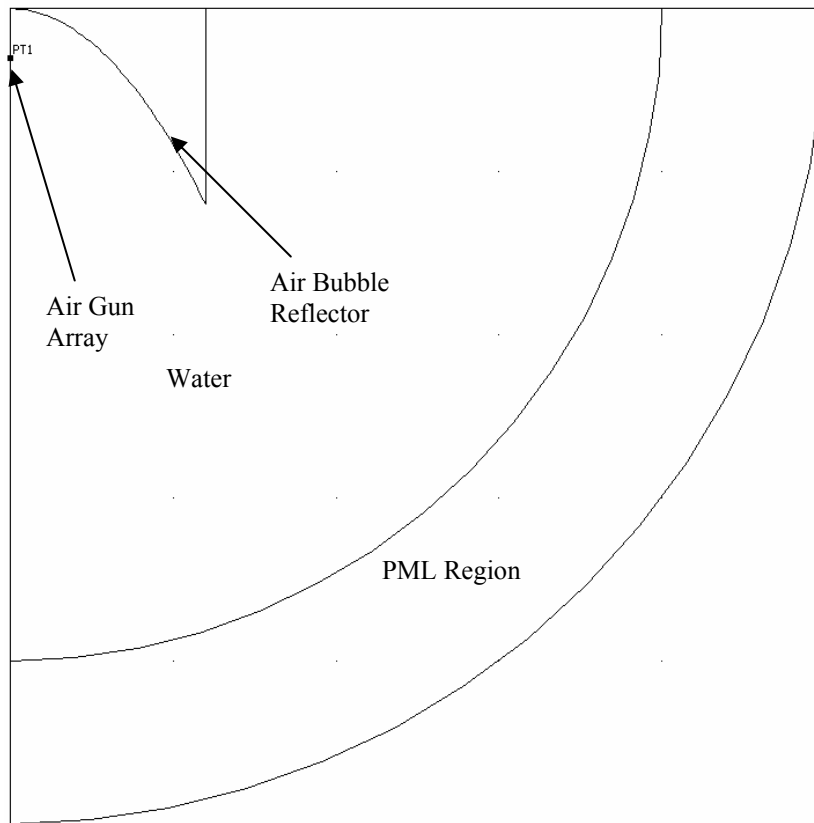


FIGURE 28: Lateral Directivity for Single Line Air Gun Array, 3 Meter Depth, No Reflector

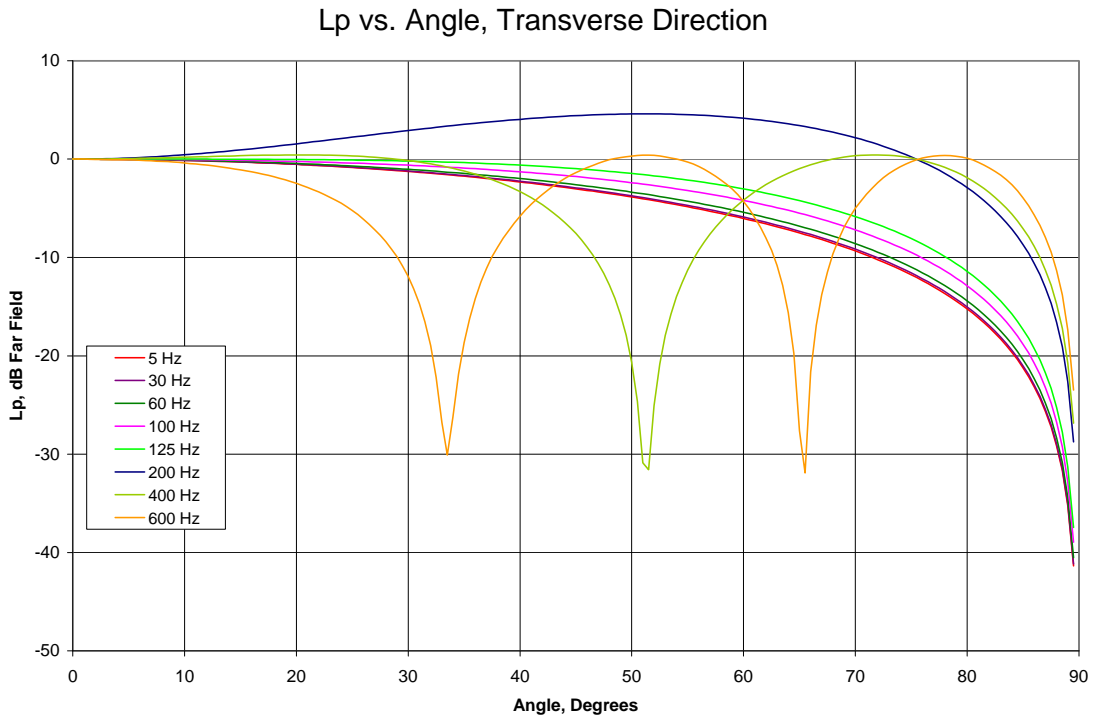


FIGURE 29: Reflector Effectiveness, 3 Meter Deep Array, Large Reflector



FIGURE 30: Reflector Effectiveness, 3 Meter Deep Array, Medium Reflector

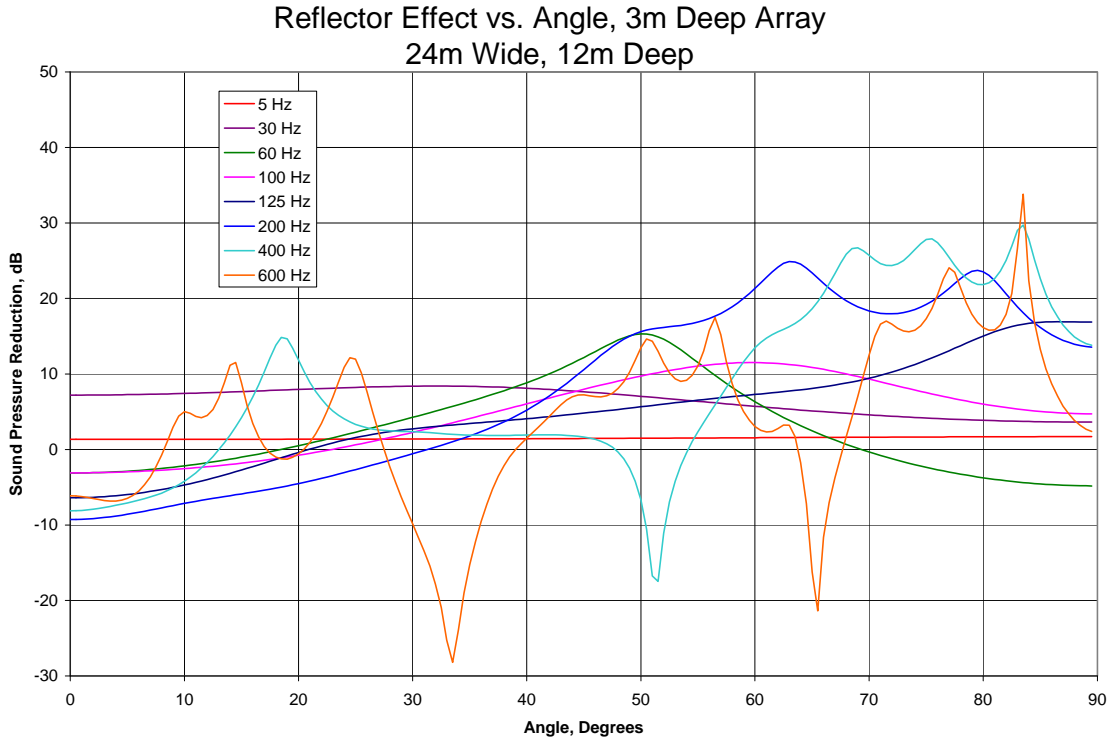


FIGURE 31: Reflector Effectiveness, 3 Meter Deep Array, Small Reflector

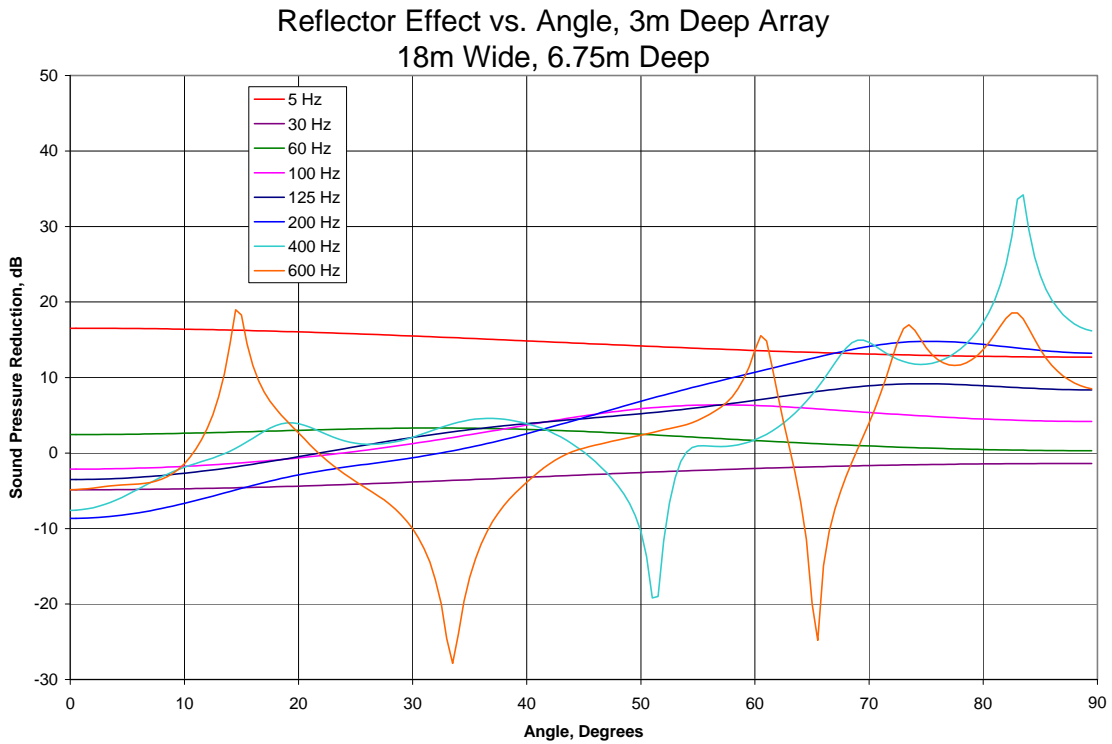


FIGURE 32: Reflector Effectiveness, 6 Meter Deep Array, Small Reflector

Reflector Effect vs. Angle, 6m Deep Array
24m Wide, 6m Deep

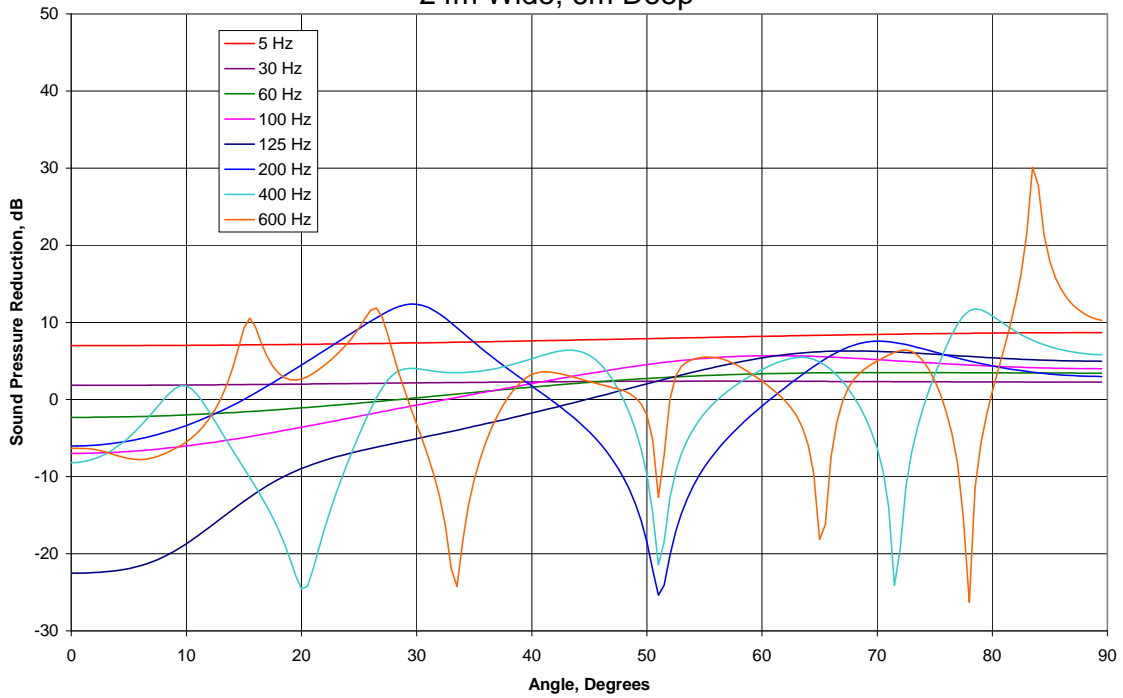


FIGURE 33: Reflector Effectiveness, 3 Meter Deep Array, Medium Reflector, 30 Meter Deep Water (Shallow)

Reflector Effect vs. Angle, 3m Deep Array, Shallow Water
24m Wide, 12m Deep

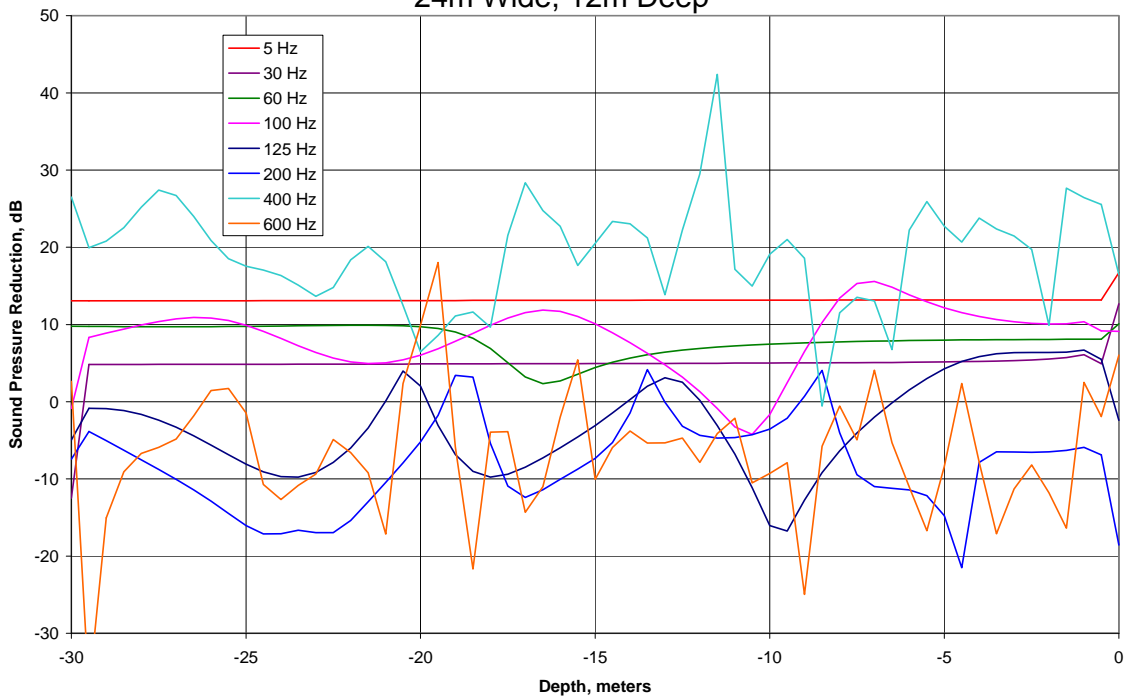


FIGURE 34: Reflector Effectiveness, 3 Meter Deep Array, Medium Reflector, Pressure Release Surface

